Interface Characteristics of Laser Impact Welded Aluminum-Steel Spot Welds

By
Katrin Daehn
The Ohio State University, Columbus OH 43221

Honors Thesis Advisor
Dr. John Lippold

Abstract

Laser impact welding (LIW) is a novel solid-state technique for spot welding a foil onto a substrate at millimeter-length scales. This process can minimize the formation of continuous intermetallic phases and heat affected zone, allowing for the joining of dissimilar metals. In LIW, a plasma forms under a confinement when the laser is pulsed, accelerating the flyer metal to a great velocity over a short standoff distance to the target material. With proper impact conditions, a plasma jet is formed at the collision point that strips the flyer and target material from oxides and other contaminants. Interatomic bonding occurs when these two clean surfaces meet under pressure. Due to high strain rate deformation as well as possible local melting, diffusion, and mechanical alloying, the interface can exhibit grain refinement, intermetallic phases, microvoids, twinning and high dislocation density – all which will affect the overall properties and heat-treatment behavior of the weld, and have not been thoroughly studied in LIW. An investigation of these interface characteristics in the historically difficult to join system, aluminum-steel, will be conducted. A YAG laser was used to aluminum-steel under specified impact angles and the impact velocity was measured using a Photon Doppler Velocimeter system. Optical microscopy and SEM study shows an unsymmetrical flat-wavy interface with pockets, as well as layers, of intermetallics. Thick intermetallics are often accompanied by voiding. Regions showing evidence of local melting and resolidification were observed. Nanoindentation revealed some annealing of the aluminum flyer, which was originally in the full hard temper. Flyer thickness tearing was the only observable effect changing impact angle had, and no patterns in microstructure or weld quality were noted as impact angle varied. Heat treatments were conducted and there were differences between what would be expected from interdiffusion of an unbonded couple, showing that the interface characteristics imparted from collision had an effect on the growth and reactions occurring during heat treatment. Phase identification analysis is needed to better understand the heat treatment results. Reproducibility between welds was a significant issue and future work involves standardizing the procedures to better determine the variables causing the interface observations. Understanding the LIW technique will be valuable for medical, electrical, battery and automotive industries.

Acknowledgements

Many thanks to Geoff Taber for his help in operating the laser, creating welds and for his valuable insight. He was absolutely essential in helping me produce the samples to investigate. Thank you to David Tung and Dr. Huimin Wang for their involvement in using the SEM and for their thoughts as we examined the microstructure. I really appreciate the time David Tung put into SEM analysis. Thank you to Marc Doran for performing nanoindentation with me, teaching me how it worked and for his insight on my results. Thank you to my advisor, Dr. Lippold, for the project idea and for his insights and pushes along the way.

Introduction

Laser impact welding (LIW) is a novel solid-state collision welding process that can be used to create spot welds between a foil and substrate at millimeter-length scales. In solid-state welding, the temperatures at joining are lower than the base material melting points. Liquid state welding (e.g. fusion welding) has been widely developed and relies on heat input to produce a liquid phase at the interface between two base metals. The properties of the base materials can be degraded in the Heat Affected Zone (HAZ), due to residual stress and consequent cracking and corrosion issues. Additionally, fusion welding is largely limited in the systems they can join, particularly in dissimilar systems. Dissimilar weld systems for fusion welding must have similar melting points, thermal expansion coefficients and thermal conductivity. Meeting these requirements, the bonding mechanism still often produces brittle intermetallic compounds at the interface, which can then cause brittle failure in the weld. LIW can avoid many of these issues because bonding occurs in the solid-state. There is no significant melting of the base metals and there is little heat input if any, so the properties of the base materials are retained or even improved due to the refined structure. Similar and dissimilar materials can be joined regardless of property differences. Theoretically, LIW can be used to join any two metal systems. Within dissimilar systems joined with LIW, the formation of intermetallic compounds is limited and often not continuous due to the low temperatures and extremely short times involved in joining. As automobiles, aircraft and bicycle manufacturers strive to create optimal lightweight structures, it has been recognized that these often require many different materials, which must be effectively joined [1].

LIW is the first use of the high velocity collision welding technique used at millimeter length scales. The joining mechanisms are novel and result in the limited formation of intermetallics, which is a very important criterion. However, since the collision process involves severe plastic deformation and high strain rate induced-fluid like behavior in the base materials, other important microstructural features will invariably result at the interface. These must be understood. These interface characteristics have been studied in detail at different length scales, but not yet thoroughly in LIW. LIW in particular is a method well-suited for the assembly of micro-devices, such as in micro-electronics, medical devices and batteries [2]. Understanding what microstructural features can be expected at LIW dissimilar welds and the parameters affecting those features is of great importance. In this study, the interface characteristics of LIW-produced welds in the historically difficult system, aluminum and steel, will be investigated using optical microscopy, SEM, nanoindentation and heat treatments.

Literature Review

Solid-State Welding

Many solid state welding methods have been developed, such as friction welding, friction stir welding, diffusion welding, ultrasonic welding, roll welding, explosive welding, magnetic pulse welding, laser impact welding and gas gun welding. Solid-state welding involves bringing two surfaces in atomic contact with each other. Surface asperities, oxides and contaminants often prevent the direct contact of atoms, but these are broken down in solid-state welding processes through surface preparation, plastic deformation and heat [3].

Ultrasonic welding is commonly used in industry to join small electrical contacts between dissimilar metals in electronics and computers. It is useful to compare LIW to ultrasonic welding because of their similar applications. In ultrasonic welding, due to the friction between the two materials, the oxides on the surfaces break into small pieces. In the positions where nascent surfaces are created and in contact metallurgical bonding occurs. When joining hard-soft dissimilar metal combinations with ultrasonic welding, higher weld times and energy are required. Generally the rapid weld cycle in ultrasonic welding prevents the formation of an intermetallic layer, but in joining combinations such as aluminum and steel, the high energy input can lead to significant interdiffusion between the base materials and an intermetallic reaction layer. In joining 1mm thick aluminum and steel sheets for the automotive industry, it was found by Pragnell et al. that the dominant factor limiting the joint strength was a thin <2 μm intermetallic reaction layer, which reverted the failure mode to cleavage at the interface [4].

High-Velocity Collision Welding

Explosive welding (EXW), gas gun welding, magnetic pulse welding (MPW), vaporizing foil actuactor welding (VFAW), and LIW feature high impact velocity, but at greatly varying length scales. EXW is suited for large planar interfaces, up to meters in length, but due to the dangerous explosions involved it is confined to isolated settings and is difficult to incorporate into industry. MPW can provide linear or circular welds, but on the order of meters or less, with typical widths of millimeters to centimeters. MPW uses electromagnetic force to accelerate the flyer plate. MPW uses an electromagnetic field and thus the flyer plate must be electrically conductive and plastically deformable, or coupled to a conductive driver. Vivek et. al reported a novel method for implementing collision welding at length scales similar to magnetic pulse welding using a vaporizing foil actuator in VFAW [5]. LIW creates spot-like welds on the order of millimeters in diameter. The optical output energies for LIW are in the order of a few joules, as opposed to several or tens of kilojoules for MPW and megajoules for EXW [1, 6]. MPW,

VFAW and LIW have been reviewed as realitvely simple to integrate into factory environments [6]. These are useful collision processes to understand and compare to as many of the same mechanisms and resulting morphological and microstructural weld features are similar.

LIW Process

In LIW, a thin ink layer is applied to a flyer material, providing the flyer with an optically absorbant surface. A transparent confinement is placed over the flyer. When the laser is pulsed, it travels through the confinement and the ink on the foil ablates. The ink layer absorbs the laser's optical energy, creating plasma. The confinement contains the plasma-based pressure, accelerating the light flyer metal to a great velocity over a short standoff distance to the target material. At the right impact angle and impact velocity, jetting occurs at the collision point, which scours the surface clean of oxides and contaminants during impact. Metallurgical bonding by oblique impact of the clean surfaces is realized and the two base metals co-deform [2].

Joining Mechanism in High-Velocity Collision Welding

In these processes, joining is the result of an instability associated with jetting. Bahrani et al. and Ezra established the impact welding principle that says when two metal plates collide at the correct velocity and angle, a jet forms at the collision point. At this collision point the impact stress surpasses the yield stress allowing the jet to propagate along the interface. The surfaces are atomically cleaned of oxides and other contaminants. When the two atomically clean surfaces meet under high pressure, bonding occurs [7]. The main essential joining mechanism in high-velocity collision welding is jetting, but intermetallic phase formation, local melting and rapid solidification, atomic diffusion at locally high interface temperatures and extensive mechanically alloying may also occur and aid in bonding the two base materials [1]. The collision process often involves severe plastic deformation, mechanical alloying, possibly local melting with rapid solidification, and high strain rate induced fluid-like behavior [8].

Characterisitics of High-Velocity Collision Weld Interfaces

Microstructural evolution of the base materials at the interface occurs upon collision. This can include composition change across the interface, grain refinement, higher dislocation density, twinning, amorphous materials, microvoids and intermetallics. Generally, because the material has suffered high levels of plastic deformation with strain rate, the microstructure is quite refined and significantly higher than the base material. This is significant because in fusion welding, local heating generates heat affected zones that are almost universally softer than the base metals, which reduces joint efficiency. Existing grains near

the mating interface are extensively elongated along the welding direction. The grain refinement and grain elongation can significantly influence the hardening. However, local heating may also introduce recovery or recrystallization.

The interfaces are generally highly heterogeneous. From the collision point to the entire mating surface, the velocity distribution, the strain and strain rate distribution have large variations [6]. The heterogeneity is also partly due to varied instabilities including Kelvin-Helmholtz instabilities, which induces dynamical shear stress and shear strain flows along the welded interface. This is believed to be the mechanism critical for the development of wave morphology [9]. Interfaces, especially in LIW, can be straight or wavy and the transition from a planar to a wave interface appears to be related to an increase in the plastic strain and shear stress, as higher plastic strain and shear stress are seen for wavy interfaces [1]. The temperature rise at the interface encourages wave formation by softening of the interface and its vicinity [10].

The interface temperature has not been experimentally measured, so it is not known the extent to which temperature rises upon impact. However, it is possible that significant heat is developed on impact between the flyer and the base – often sufficient to cause local melting. This can aid in the formation of intermetallics, which have been noted in various collision welding processes. These often occur in discontinuous pockets, especially at the vortices of waves. These pockets of intermetallics are likely formed by intense local heating, melting, mixing and rapid solidification. Most welded region is free from intermetallic phases in all cases. The increased interfacial temperature, coupled with the concentration gradient at the interface can cause interdiffusion, but this is often not likely due to the extremely short impact times. Thus, composition gradients outside of intermetallic formation are not normally observed [1].

Important Parameters in Collision Welding

Jetting is essential for bonding in high-velocity collision welding. The metal plates must collide at the correct angle and velocity for the impact stress to exceed the yield stresses of the base materials and propagate the jet along the surface. Thus, impact angle and impact velocity have found to be crucial parameters in collision welding. With a fixed impact angle, the impact velocity has a dominant effect. Excessive velocity can cause significant melting, leading to intermetallic formation, or it can produce brittle damage or spalling in the impacting plates. Insufficient impact velocity may not initiate the jet required to remove the surface oxide [1]. Collision welding of a given pair of metals occurs only when the collision angles and velocities are within an optimum range, called the welding window. Successful collision welds are generally obtained with the collision

velocity is in the range of 150-1500 m/s and the collision angle is between 5º and 20º. The properties of the colliding materials have a significant affect on what the welding window will be. The higher the yield strength of the materials, the more difficult jet initiation will be and interface features such as wave formation will be affected by how hard and dense the materials are [10].

In LIW, confinement layer can have a significant impact on the resulting impact, as it controls the plasma pressure. When there is free space between the confinement layer and the ablative layer, the plasma is not controlled in one direction. In a comparison between conventional soda-lime glass, microscope slides and polycarbonate all attached to the substrate and flyer set up with tape, polycarbonate was chosen because it does not break and is easy to work with. However, in scaling up to industry, it was suggested that a thin water layer over the flyer would be the best confinement [3].

In LIW, the laser energy can be varied between the nominal values 0.216 J, 1.0J, 2.0J, and 3.0J. Keeping all other variables constant, energy was not found to have a dramatic influence on the acceleration or impact velocity of the flyer. The diameter of the laser beam can be adjusted by changing the distance between the focus lens and the experimental set up. This proved to be an important paramter as changing the laser spot size varies the energy density, which affects the impact velocity of the flyer. The impact velocity increases with increased laser energy density. Damage to the flyer can occur with the energy density is too high [3].

Geometry of the joint can also have a significant influence on the interface characteristics. Flyer plate thickness will influence the wave shape, wavelength and the amplitude [11]. The wavelengths and amplitudes increase with sample thicknesses [6]. Since flyers of varying thicknesses have different masses, their acceleration and impact velocity vary. Impact velocity decreases with flyer thickness. The standoff distance between the flyer and substrate is not always a significant variable. It has been measured that the acceleration process takes place in 200 nanoseconds, with a displacement of 60 microns. After this distance, terminal velocity is reached and maintained for several millimeters. Thus, as long as the standoff distance is sufficient to allow for complete acceleration, about 60 microns, and does not exceed several millimeters, the resulting weld should not be affected as standoff distance varies.

LIW Findings

Alexander et al [12] used an experimental set up where the ablative layer is 0.5 micron thick Al deposited on glass and the flyer was 1 micron thick Al deposited on the first layer. The flyer was set in direct contact with the target. Melting and resolidification was observed for the Al-Cu weld and higher laser power was

needed for welding aluminum and silicon. The experiments were under vacuum, which resulted in reduced trapped air at the weld interface.

Dubrujeaud and Jeandin [13] used 20 micron thick Al onto grooved Al2024 where the impact angle was controlled to be 16.7º. The experiments were under vacuum. At the bottom of the groove, melted and solidified zone appeared. Along the edge, there was a wavy interface and the amplitude increased with the depth of the groove. At the highest point of the groove, no melting or waviness was observed. Barradas et al studied aluminum and copper and observed intermetallics. Metallurgical bonding occurred along edges of the spot [14].

Zhang et al. welded AA1100 plates and low carbon steel 1010 plates with LIW. The flyer sheet had a thickness of 0.175 mm. The impact angle was 15º. Metallurgical bonding and hardness increase at the interface was observed. The interface had small, inconsistent waves and no intermetallics were observed [1].

Wang studied the laser impact welding application in joining aluminum and copper and aluminum and titanium. Using a standoff between the flyer and substrate with no direct impact angle, the characteristic morphology for the geometry was an annular ring about the center of the beam because the impact angle was satisfied at the edges. In the center of the spot, entrapped metal is observed, probably the result of metal jetting. In Al-Ti, discontinuous intermetallics were observed at the interface about 5 microns long and 1 micron thick. Lots of voids were observed along the interface and twinning was observed in Ti accompanied by a hardness increase. The wavelength and amplitude varied along the weld interface. The wavy interface with relatively long wavelength and high amplitude was formed in Al-Cu LIW samples. In comparison, the high yield stress of Ti results in smaller waves in Al-Ti samples [15]. The yield stress of the target material has important influence on the morphology of the wavy interface. The SEM back scatter image didn't show any diffusion between the base materials [3].

Methodology

First LIW Configuration, Expanding Possible LIW Systems

The LIW experiments were conducted using a customized version of a Continuum Powerlite Nd:YAG laser, shown in Figure 1. The final pulse energy produced by the laser was 3.0J with a pulse width of 8.1 ns and a laser beam diameter of 12mm. Using a focusing lens, the laser beam diameter could be focused from 4mm to 2mm, depending on the distance of the sample from the focusing lens. In the first set of experiments, this was maintained at 3mm. The energy distribution from the beam was uniform and had a top-hat profile, which is shown in Figure 1.

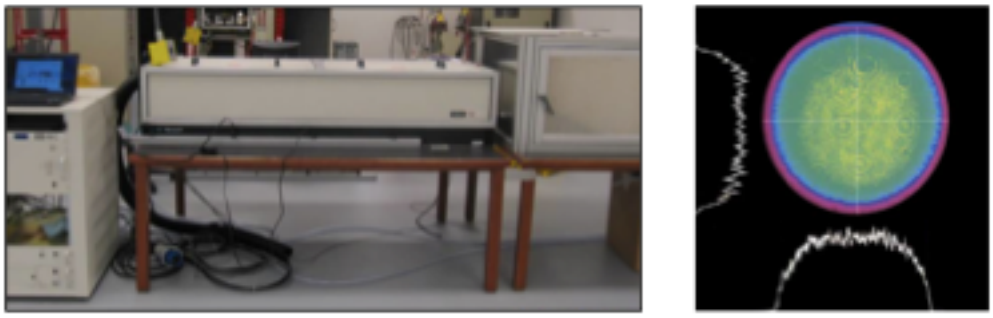

Figure 1: LIW system and energy distribution of laser beam [15]

The flyer material used was 0.002” thick commercially pure shim stock aluminum. In the beginnings of work in trying to expand LIW to more difficult systems, 0.002” thick low carbon steel, and 0.003” thick commercially pure Ti were used as well. The substrate used was 1018 low carbon steel in all dimensions large relative to the flyer. The flyer was painted with black RUST-OLEUM enamel and 3mm diameter circular samples of the flyers were cut using a sample punch. The circular flyer samples were attached to transparent borosilicate glass using annular 60 μm thick Kapton® stickers. The glass with flyers was attached to the target material using tape around the edges. The configuration can be seen in Figure 2. Both the target and flyer materials had been sanded to 600 grit and cleaned using ethanol.

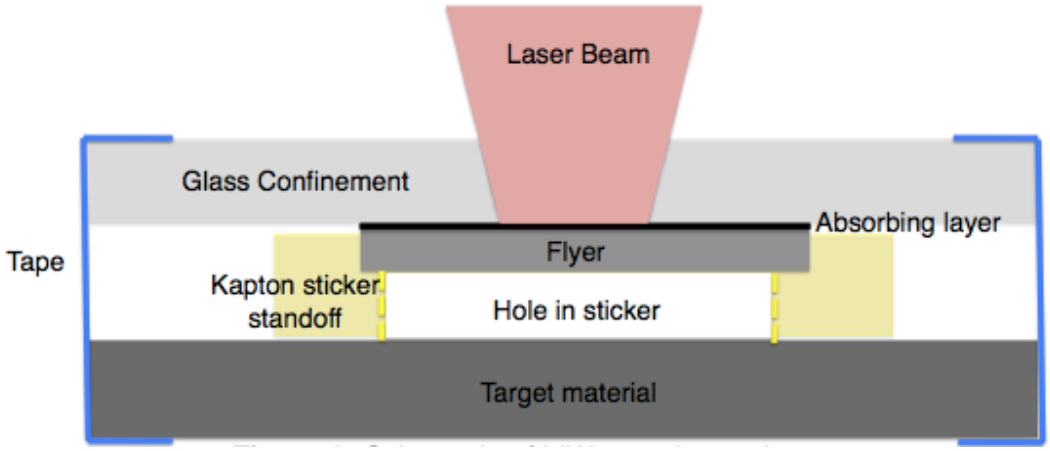

Figure 2: Schematic of first flyer-substrate configuration

Metallographic Preparation

Weld samples were cut approximately in the middle using the Tech-Cut saw. They were mounted in Bakelite, ground and prepared using normal metallographic procedures. Each sample was prepared to a 1μm polish. Most images were taken in the as-polished condition, but to reveal grain structure 5% Nital etch was used in some cases.

Second LIW Configuration for Impact Angle Identification

The flyer-substrate configuration was modified to allow for the impact angle to be directly measured. This configuration is shown in Figure 3. The angle was formed by curling the flyer with tweezers and taping the other end of the foil onto the substrate. The angle was measured by taking a picture of the flyer and substrate and using the angle measure function in ImageJ. In this set up, water-based gel was used as the confinement instead of glass. RUST-OLEUM spray paint was again used as the ink layer. In these experiments, the laser spot size was ~2.7 mm.

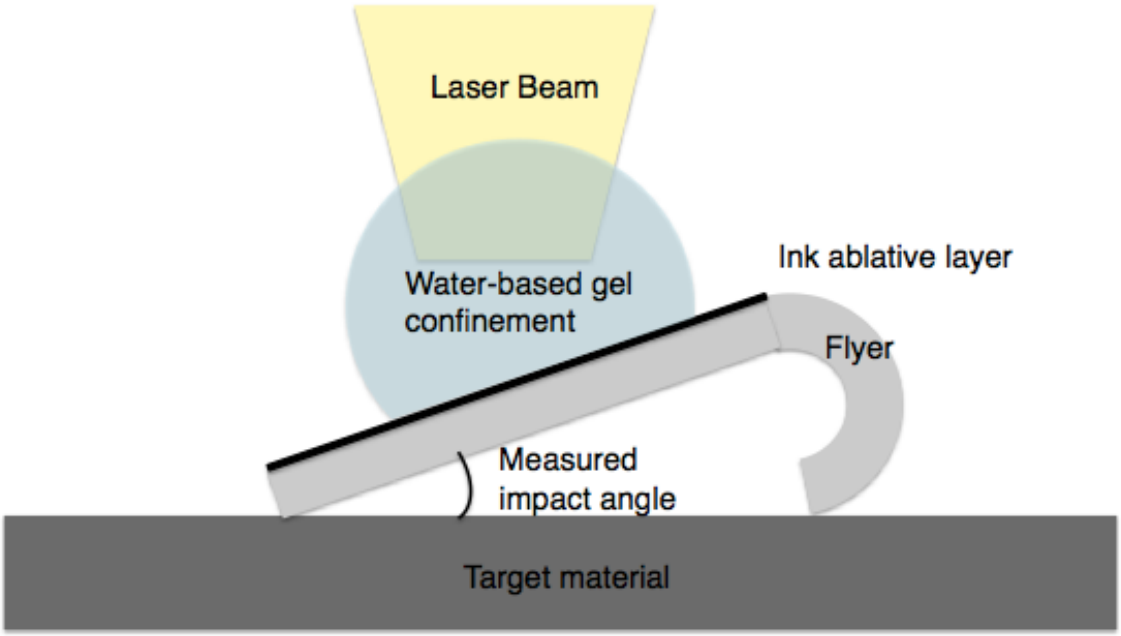

Figure 3: Schematic of second flyer-substrate configuration

A variety of welds were formed as impact angle changed. Table 1 shows the impact angles of the welds created. Welds representative of the full range were selected, cross-sectioned and metallographically prepared.

Table 1: Impact angles of welds created

High angles (°)	Medium angles (°)	Low angles (°)
25	15	10
21	15	8.5
20	14	8.5
20	14	8
20	14	7.5
19.5	14	7
18	13	6
18	12	
18	12	
	12	
	11	

In this configuration, using Photonic Doppler Velocimetry, the impact velocity of 0.002” Al was found to be ~670 m/s. There was a displacement of 60 microns during acceleration over 200 ns. Once ~670 m/s was reached, this velocity was maintained for several millimeters.

Nanoindentation

Nanoindentation was performed on two LIW samples at the interface as well as on a control piece of Al flyer that had been mounted on its side and polished to 1 μm. It was displacement controlled with a depth limit of 800 nm. A Berkovich tip was used. The LIW samples had been polished to 1μm and then etched with 5% nital. This provided surface roughness on the steel and the results were not acceptable. However, the aluminum and intermetallic areas should have provided reasobable hardness results.

Heat Treatments

Since phase identification techniques such as TEM and EBSD were outside of the scope of this present study, the heat treatment conditions were selected so that experimental results could be easily compared to literature for phase identification. A study by Springer et al. was chosen as a literature comparison. In that study, solid/solid interdiffusion was conducted at 600ºC for 1 hour, 2 hours, 4 hours, 8 hours and 16 hours. Thus, heat treatments in this study were conducted at 600ºC for 1 hour, 2 hours, 8 hours and 16 hours. Four welds (two high angle, 15º, and two low angle, 9º) were produced under the same conditions explained in configuration 2 and used for each heat treatment. The control samples (four high angle welds and four low angle welds) were produced under these conditions as well. The samples were heat treated packed in carbon in a box furnace at 600ºC.

Results

Expanding the Possible LIW Systems

First aluminum-steel welds were created with no angle between the flyer and the standoff material using the first configuration in Figure 2. Due to rebound and lack of the proper impact angle, bonding did not occur in the center of the flyer. However, annularly around the edges where the standoff provided a correct impact angle, bonding was observed. Figure 4 shows the weld cross section of 0.001" commercially pure shim stock aluminum bonded to low carbon steel (at a spot size of 3mm), as well as SEM images of the metallurgical bonding.

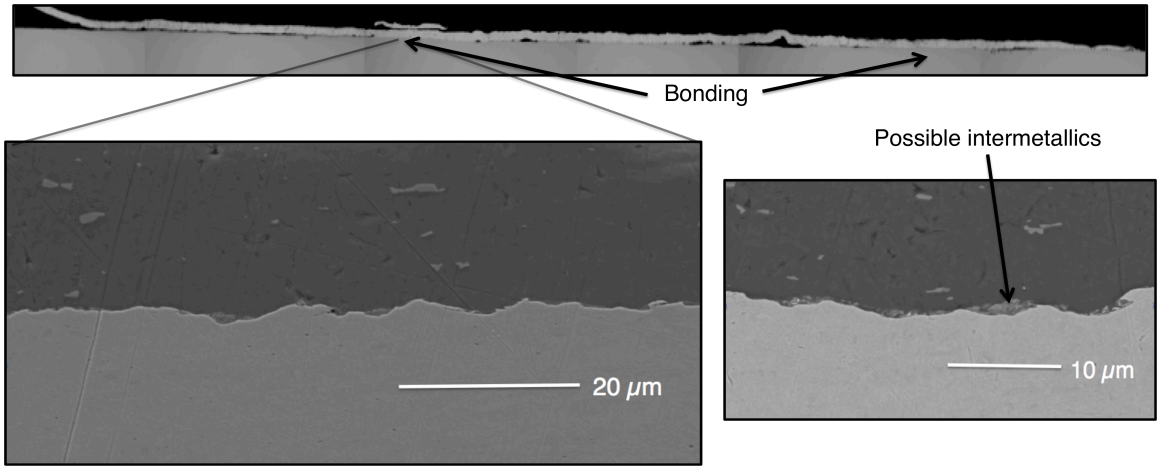

Figure 4: Bonding at interface for 0.001" Al welded to low carbon steel as revealed by secondary electrons (left). The electron backscatter image (right) reveals pockets of thin possible intermetallics.

The interface shows shallow, non-uniform waves. Within the pockets of the waves lies a phase of different contrast from the aluminum and steel as revealed by BSE. This thin reaction layer is discontinuous, is a maximum of 2 μm thick and is likely an intermetallic compound or mixture of compounds.

In the beginnings of this study, the goal was to study the interface characteristics in several different material systems, including steel-steel and steel-titanium. Only a limited number of material systems have been studied (Ni-Ni, Al-Cu, Al-Ni, Al-Ti, Al-steel and Al-Al) [15, 3, 6]. These systems feature low density flyers with a low modulus of elasticity. The beginning goals of the study were to see the interface characteristics in stiffer, denser material systems. Though LIW can theoretically join any two metals, it is well known that the yield stress of the target material has important influence on the formation of the wavy interface and that hardnesses and densities of both members of the colliding material pair affect the

welding window [15, 17]. Furthermore, a higher density flyer is more mass for the same dimensions and is more difficult to accelerate. Thus, there are likely intrinsic limitations in expanding LIW to more difficult systems using flyers and targets that are more dense, stiff and strong.

Welds were not achieved when 0.002” thick low carbon shim stock steel was used at the flyer, as well as when 0.003” thick commercially pure titanium was used as the flyer. The configuration described above and shown in Figure X with no impact angle between the flyer and the target substrate was used. In these tests the ablative ink was the black RUST-OLEUM enamel and the confinement was the borosilicate glass.

In order to better deform higher density and stiffer materials, a new process was developed. In this process, the optical energy from the laser was augmented using nitro methane mixed with carbon black particles. Instead of using the black enamel as the ablative layer, a mixture of nitro methane and carbon black particles was deposited on the surface of the flyer beneath the glass substrate. Significantly greater deformation of the flyer and target was observed, however, welds were not reliably produced and steel-steel and Ti-steel welds were still not produced using the flyer materials described above. Figure 5 shows deformation of the Ti flyer from nitro methane augmentation, and the deformation typically seen using the original process.

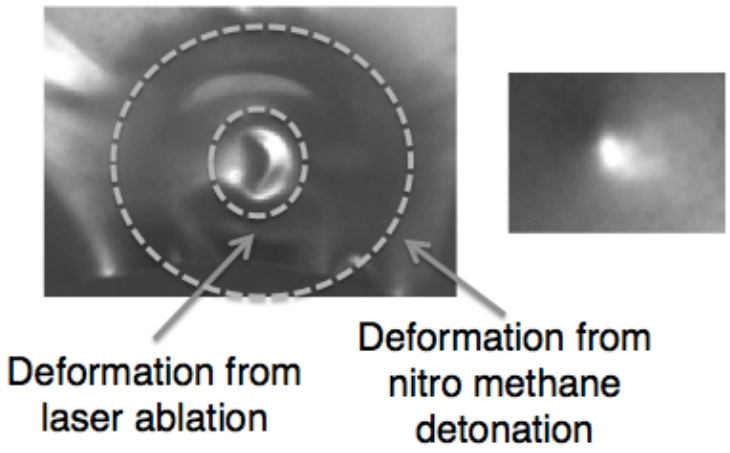

Figure 5: Deformation of Ti flyer with nitro methane (left) and from using original process without augment (right)

From the flyer deformation, it was hypothesized that the laser ablation and nitro methane detonation were not occurring at the same time. Bonding takes place during impact from plasma acceleration of the flyer created by the ablation of the optically absorbent layer. If the detonation of the nitro methane were taking place after this, it would not be aiding in the bonding process. Instead, it is likely that

the nitro methane is simply serving to further deform the flyer material. However, it is possibly increasing the impact velocity in the bonding regions. Figure 6 shows SEM images of bonding at the interface for 0.002" Al welded to low carbon steel using the nitro methane augment. As can be seen, the waves have a higher frequency than was observed in Figure X with the original experimental setup. Several waves show vortices and there are pockets of intermetallics. The appearance of porosity and voids along the interface and in the intermetallic pockets suggest that local melting and resolidification occurred. Increased impact velocity is known to cause melting and intermetallic formation [1], so it is likely that the nitro methane augmentation is increasing impact velocity.

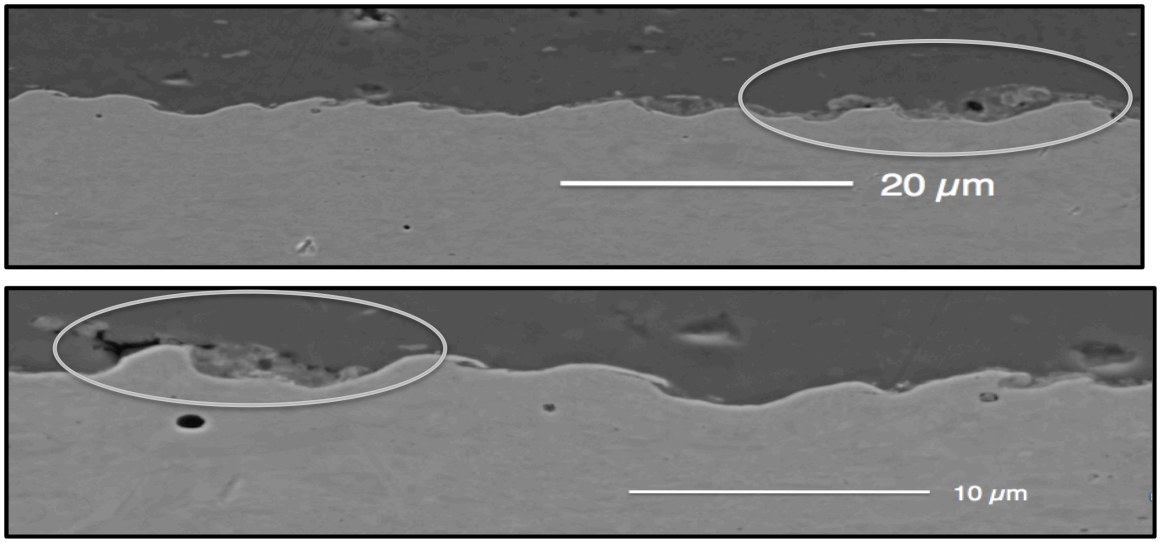

Figure 6: SEM secondary electron images of bonding at the interface for 0.002" Al welded to low carbon steel using nitro methane as augmentation. The circled regions show where possible local melting and resolidification occurred.

More investigation is needed to understand the impact progression between the ablative energy and the nitro methane detonation. Photonic Doppler Velocimetry (PDV) tests can be done to determine how the nitro methane detonation is interacting with the flyer impact. Upon this understanding, it will be known if the nitro methane is serving to increase impact velocity. Increased impact velocity may help to expand the welding window and thus the range of materials that can be produced using LIW. From the observations in this study, preliminary thought is that the nitro methane was detonating after bonding took place and it was only serving to further deform the flyer and input heat into the system.

In expanding LIW to higher density, stiffer systems, the nitro methane method shows that there is yet much room for innovative strategies to improve the laser-driven flyer system – in the confinement layer, connection between the confinement layer and flyer and in the ablative layer. Improvements in these areas could increase energy efficiency and the impact velocity of the flyer.

However, there may exist some fundamental limits and some systems may not be feasible in LIW whatever the welding window.

When the flyer does have a high density, it is important that the dimensions are smaller and scaled to accommodate for the higher mass. 0.002” steel and 0.003” Ti were used in this experiment. These thicknesses are suitable for Al, but not for these more dense materials. The next step in determining the feasibility of using LIW with those flyer materials would be to use a flyer thickness of at most 0.001”.

Interface Characteristics of Al-Steel LIW welds

Though further adjusting the laser-driven flyer system and changing the parameters to allow for the bonding of more material systems is important, a fundamental understanding of the interface characteristics in LIW-produced welds was needed. It was decided to focus on the interface characteristics in LIW spot welds of commercially pure shim stock aluminum and 1018 low carbon steel for the duration of the study. Iron and Aluminum rank among the most important engineering materials because they provide good properties at low material costs in many applications [18]. Their joining by traditional processes is hindered by the large difference in melting temperatures, the difference in mechanical properties, and because of the formation of brittle intermetallics. Iron-Aluminum welds have been a large focus in many solid-state welding processes, including ultrasonic welding and magnetic pulse welding, which are good comparisons to LIW [4]. Additionally, Al-steel welds produced by LIW have been studied briefly before [15]. In determining the interface characteristics and bonding mechanisms expected in LIW-produced welds, it was decided that the Al-steel would be a basic, technically important system to investigate. Due previous research of Fe-Al welds done in similar processes, there would be literature to compare our findings to, to further determine the feasibility of LIW for industrial scale-up.

Defining the Welds

In defining the interfacial morphology and microstructure, it was important to first define the created welds. Impact velocity and angle have been identified as important parameters that determine the weld quality and interface [6]. The impact velocity of flyers has been studied by Wang using PDV measurements. It was found that the laser energy value does not have a significant effect on impact velocity, but laser spot size changes the energy density, which effects impact velocity of the flyer. The interface morphologies of Al-Ti LIW samples produced at different impact velocities were studied. It was found that higher impact velocities are necessary for wave formation. The configuration used in this experiment had no impact angle between the flyer and the substrate, so the impact angle at the annular bonding was not known [3].

In a study by Liu et al, a corrugated surface was made for the flyer to impact the target with a gradual impact angle from 0 to 30 degrees. Bonding was observed at small angles (7-9 degrees) and no bonding was observed at high angles (30 degrees). From those results, the optimal impact angle of 7.5 degrees was used for subsequent experiments [15]. Small and high angles were produced and observed, but the incremental angles between these two extremes were not thoroughly studied. Furthermore, the interface morphology and microstructure were not studied as impact angle varied, except for to see if bonding had occurred or not.

Bonding of Welds with Varying Impact Angles

The range of acceptable impact angles must be more thoroughly studied as it is such an important parameter for the formation of the weld and the consequent interface morphology and microstructure. To do this, a new flyer-substrate configuration was developed to easily produce a known impact angle. This configuration is described in the Methodology section and a schematic is shown in Figure 3. The advantage of this new configuration was that bonding was not limited to the annular edges. Bonding could occur over the entire spot size interface – though this did not usually happen due to jetting and other heterogeneities. The confinement used was also easier to work with and was more energy efficient than the original borosilicate glass confinement. Using this configuration, 0.002” thick commercially pure Al was bonded to polished 1018 low carbon steel substrate at a variety of angles in Table 1 in the Methodology section. The impact velocity was kept constant for the welds produced, around a measured velocity of 670 m/s. Of those welds produced, a variety of welds representative of the range of angles were selected and cross-sectioned through the center of the spot weld. Figure 7 shows the morphology of the interface of the welds as revealed by optical microscopy in the as-polished condition.

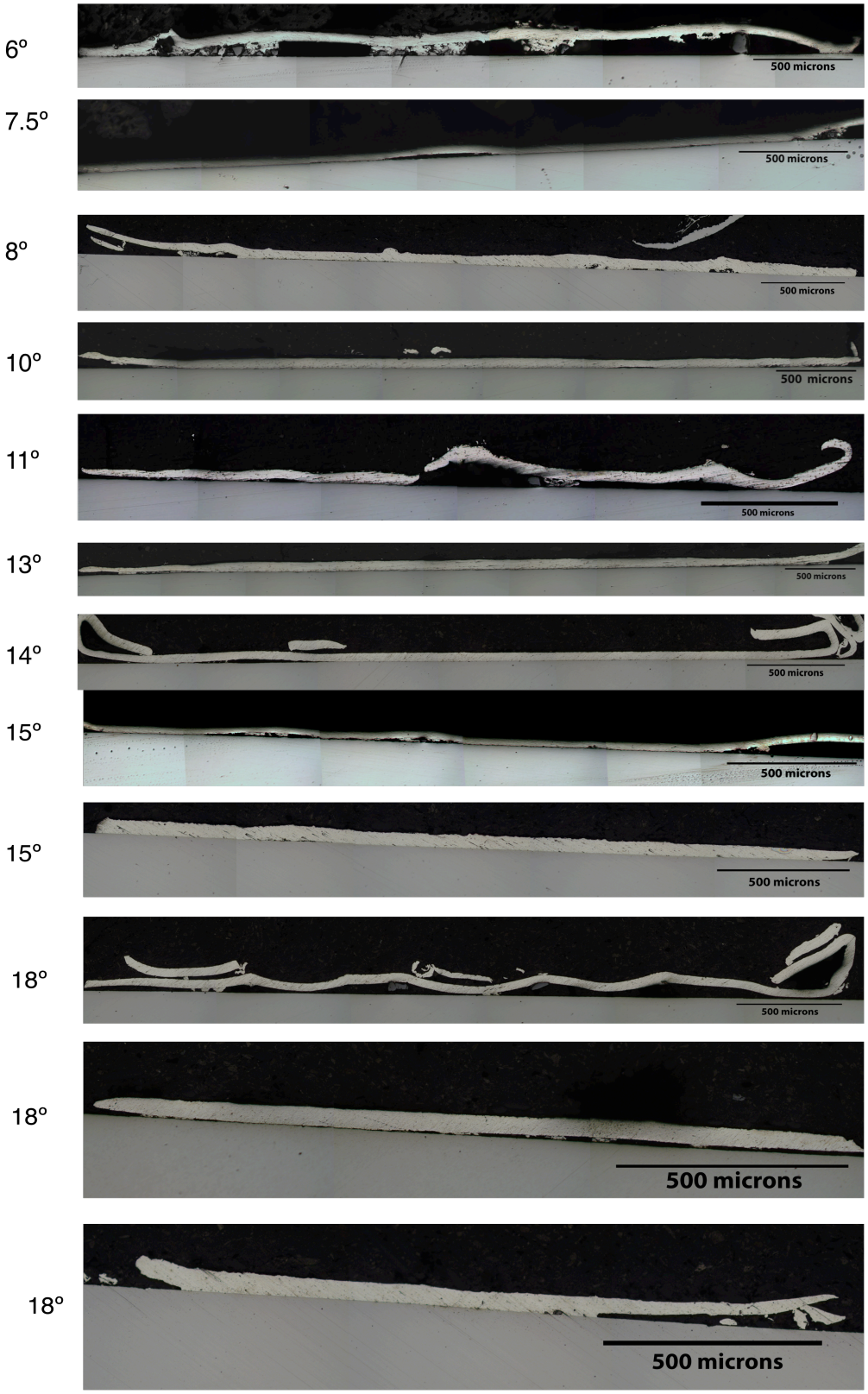

Figure 7: Morphology of 0.002” Al-steel weld interfaces created at varying impact angles as impact velocity was kept constant

Welds were successfully produced at a variety of angles. Figure 8 shows top views of a few examples of the welds produced before cross-sectioning. The general trend is that flyer damage – deformation and tearing – increases as impact angle increases. Below about 9º, the flyer stayed intact. Above 9º, there was consistently tearing of the aluminum at the border of the weld. It is known that displacement over long distances can cause the flyer sheet to deform, as well as cause heating due to interaction with the atmosphere or plasma [15, 19]. With higher angles comes a greater standoff distance, so the flyer damage could be a result of larger displacement. Alternatively, flyer damage could be taking place during impact instead of during travel towards the target.

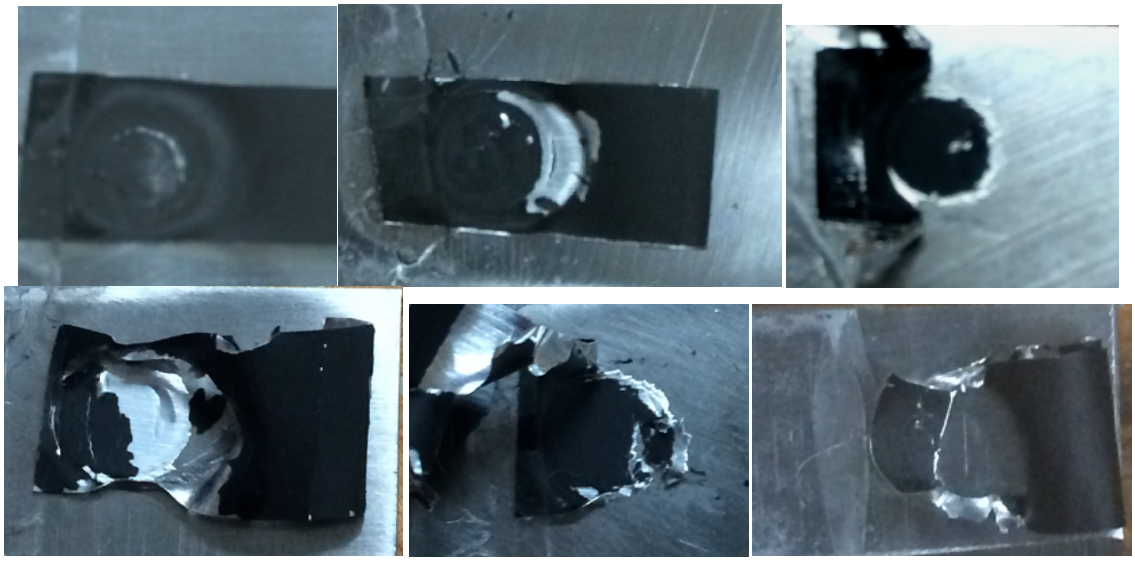

Figure 8: Top views of welds created at impact angles of (from top left to bottom right) 6º, 8.5º, 11º, 13º, 15º, and 20º.

Table 2 shows the results of the welds created at each impact angle. All welds from 6 to 18º were about the size of the laser spot. When peeled, the aluminum tore and no failure was observed at the weld interface. However, as can be seen in Figure 8, for many angles the aluminum was already partly torn around the outside of the weld, thus the aluminum would be more prone to failure even if the weld exhibited poor strength. For these reasons, a better test of the mechanical properties of LIW-produced welds needs to be developed.

Table 2: Results of welding 0.002" Al to steel at various impact angles. No comment means weld created was about the size of the laser spot and failure during peel test was in tearing of the aluminum

Angle (degrees)	Comments
6	
7	
7.5	
8	
8.5	
8.5	
10	
11	
12	
12	
12	
13	
14	
14	

Angle (degrees)	Comments
14	
14	
15	
15	
18	
18	Small Weld
18	Small Weld
19.5	No Weld
20	Small Weld
20	No Weld
20	No Weld
21	No Weld
25	No Weld

As can be seen by Table 2 and Figure 7, a large variety of impact angles produced successful welds. There is a limit at high angles, around 18º. The last two micrographs in Figure X show welds produced at 18º with significantly decreased cross-sections. Above 18º, there was no evidence of welding or material transfer with the exception of a small weld that formed at 20º. This window of impact angles is consistent with the welding windows for other collision welding processes [6, 10].

At smaller angles, welding is consistently successful, but there appears to be a limit around 6º. The first micrograph in Figure 7 shows extensive jetting entrapment, with true bonding occurring only over a small area at the edges. At impact angles below 6º, sufficient jet expulsion may not be possible.

At all impact angles safely within the window, weld reproducibility is an issue. As can be seen in the last three micrographs in Figure 7, two welds produced at 18º exhibit good bonding over a small cross-sectional area with no jet entrapment, and one weld produced at 18º exhibits extensive jet entrapment through the majority of the weld interface and bond only at the edge. Similarly, the two 15º welds show significant differences in morphology – one showing bonding over a large area and the other exhibiting large areas of voids and lack of metallurgical bonding. With such differences apparent between two welds made at the same impact angle under the same conditions, it is impossible to make conclusions about patterns in morphology (e.g. jet entrapment, bonding surface area) within the range of acceptable impact angles.

Flyer Thickness Parameter

0.002” thick Al flyer was the main subject of this study, but 0.001” and 0.003” Al fliers were welding using the same laser spot size and a 13º impact angle, which had produced successful welds for 0.002” Al. Welding these flyer thicknesses under those conditions proved unsuccessful. Figure 9 shows that the 0.001” ablated and only oxide particles were found on the surface using SEM. Figure 10 shows the cross-section of 0.003” Al welding. Extensive jet entrapment and spalling of the flyer was observed. It is well known that flyer thickness is an important parameter effecting the morphology and microstructure of the interface. The welding window changes as flyer thickness changes. Flyers of varying thicknesses have varying mass, so flyers with varying thicknesses accelerated at the same laser spot size will have different impact velocities. The 0.001” flyer is the thinnest and has the smallest mass, and would have the highest impact velocity – this proved to be too high. The 0.003” flyer had greater mass and the impact velocity proved insufficient to expel the flyer. The developed configuration can be used to find the appropriate welding window as flyer thickness changes.

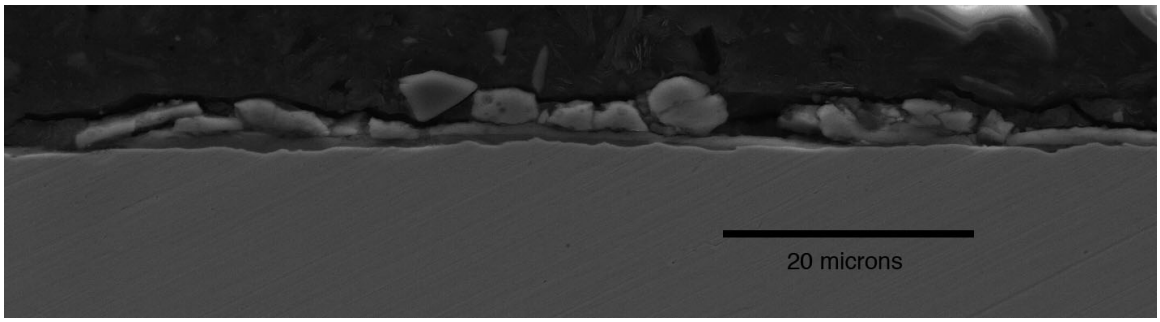

Figure 9: SEM image of steel surface after welding 0.001” Al using same impact velocity and 13º impact angle

Figure 10: Cross section of 0.003” Al welded at same impact velocity and 13º impact angle

Microstructural Features in Welds with Varying Impact Angles

A variety of microstructural features were observed at the interfaces between aluminum and steel using optical microscopy and the SEM. These consist of intermetallic layers and pockets, voiding, evidence of local melting and resolidification, wavy and straight interfaces, and grain elongation in the welding direction. These features appeared over the whole range of impact angles and nonuniformly at different points along the weld interface.

Intermetallic Layers

Intermetallics in the form of continuous layers and in discontinuous pockets were observed at the interface in welds created at a variety of angles. Not all welds exhibited intermetallic compounds, and of the welds that did have intermetallics, they were only found in selected regions along the interface. The most continuous layer was found at the interface shown in Figure 11, formed at an impact angle of 7.5 degrees. It can be seen that a number of fairly large voids are also present along the interface. The intermetallic layer does not exceed 2 μm. Most of the time when intermetallics were present, they were of the type shown in Figures 11-14. These intermetallics were observed in discontinuous pockets, found at one or two points along the weld interface, often accompanied by voiding or evidence of local melting and resolidification.

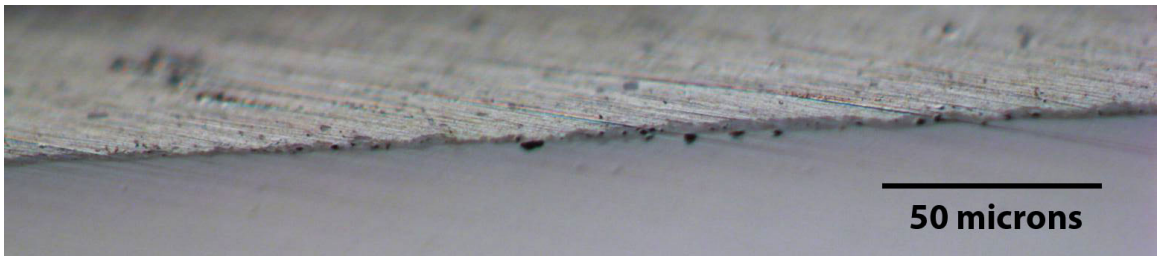

Figure 11: Intermetallic layer found in Al-steel weld with impact angle of 7.5 degrees. As polished.

Figure 12: Intermetallic pockets and voiding resembling local melting and resolidification found in Al-steel weld with impact angle of 10 degrees. 5% Nital etch.

Figure 13: Intermetallic pockets found in Al-steel weld with impact angle of 12 degrees. 5% Nital etch.

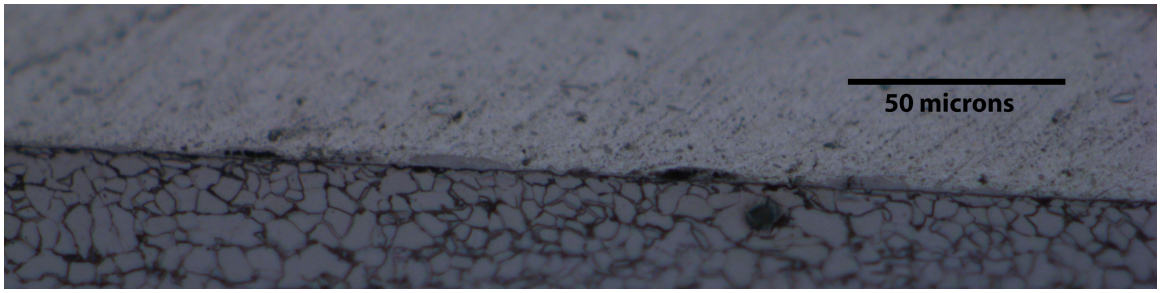

Figure 14: Intermetallic pockets found in Al-steel weld with impact angle of 15 degrees. 5% Nital etch.

Intermetallics found in a weld formed with an impact angle of 8º were examined using the SEM. Figure 15 shows the cross section of the weld from optical microscopy and SEM images taken at two different points on the interface to illustrate the vast microstructural differences that exist within the same interface. Figure 15 a) shows a region with an intermetallic layer and more waviness is in this region as well. Figure 15 b) shows a bonded region with a flat interface and no intermetallic formation.

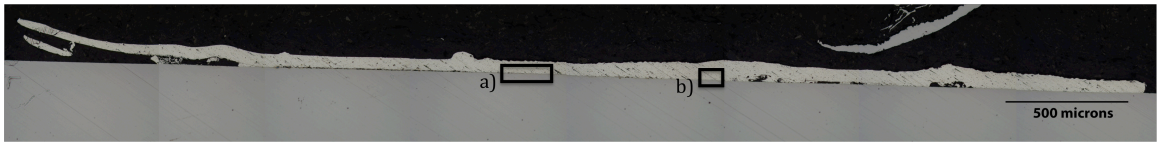

a)

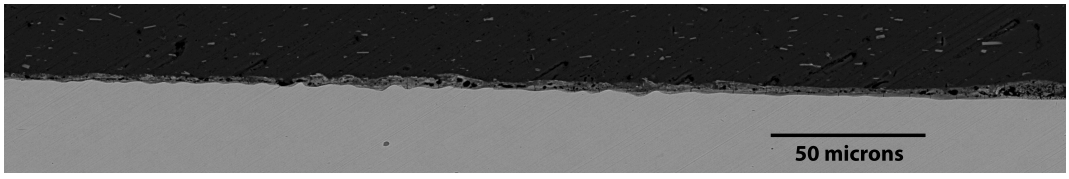

b) 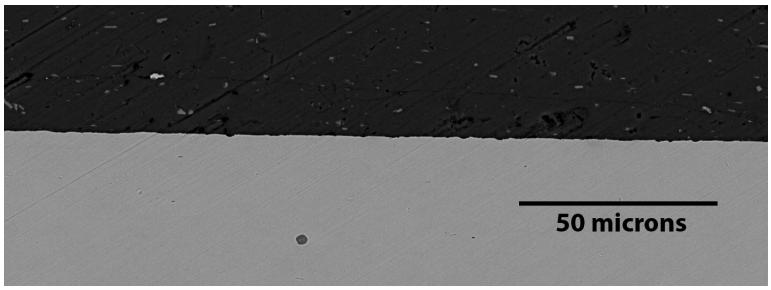

Figure 15: Optical microscopy Al-steel weld cross section in as-polished condition a) SEM backscatter image of intermetallic region b) SEM backscatter image of flat bonded region with no intermetallic formation

An EDS scan of the interface at the suspected intermetallic region confirmed that the change in contrast is due to a mixing of Al and Fe, as shown in Figure 16. This scan did not shed light on the exact compound, or whether there were a mix of fine layers of compounds or mechanical alloying occurring, but it does confirm that there is a gradient of Fe and Al concentration at the interface when there is a contrast revealed by BSE. Figure 17 shows the same region as revealed by optical microscopy. The contrast and appearance resembles what was thought to be intermetallics in Figures 11-14 above. An EDS scan of those interfaces would likely deliver a similar result and it can be well assumed that the layers and pockets in Figures 11-14 are intermetallic compounds or an alloying mixture of Al and Fe.

It can be seen in Figure 16 that the intermetallic layer is porous. It is likely that the formation of these intermetallics was aided by local melting. The interface temperature rises upon collision, sometimes liquefying the interface materials. As the liquid phases then flow around each other, intermetallics are formed upon resolidification.

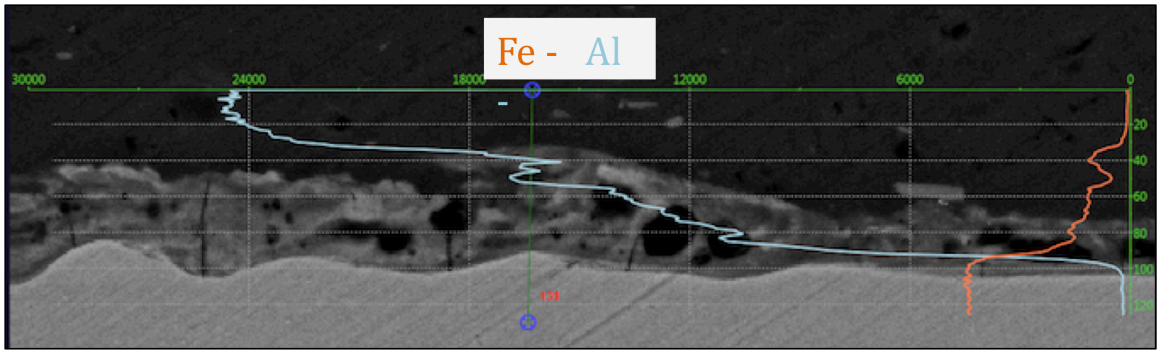

Figure 16: EDS scan of reaction layer in 8º impact angle weld

Figure 17: Optical microscopy image of intermetallic region in 8º impact angle weld. 5% Nital etch.

Local Melting

Several samples exhibited porous regions characteristic of local melting and rapid solidification. Figure 18 shows a yet different region of the 8º impact angle weld that exhibited major voiding in the reaction layer and possible local melting.

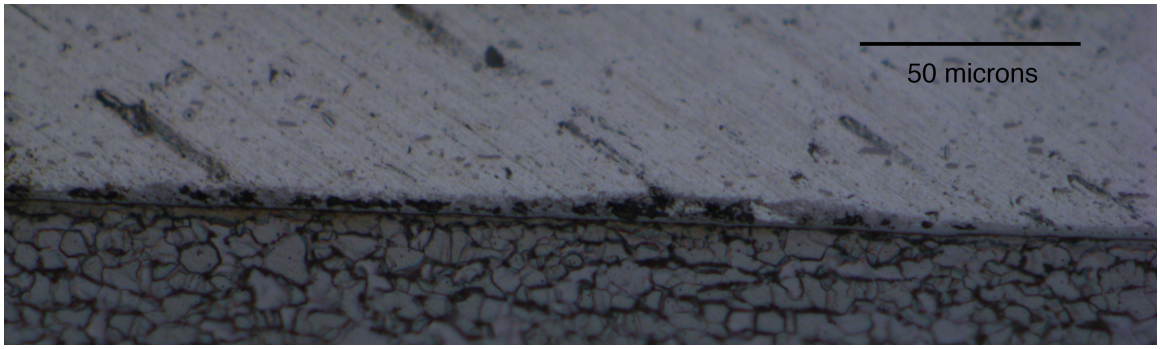

Figure 18: Optical microscopy image of 8º impact angle weld at a region where extensive voiding and likely local melting and resolidification occurred. 5% Nital etch.

Voiding in the reaction layers and in areas where metallurgical bonding occurred was seen over a range of impact angles. Oftentimes the appearance of intermetallics was accompanied by voiding at the interface, as shown in the images of intermetallics above. This may be an indication that local melting and intermetallic formation go hand in hand. It is unlikely that intermetallics form via interdiffusion due to the extremely short time of joining. Intermetallics are also observed when the interface is wavier. Higher plastic strain and shear stress are required for a wavy interface, which can cause miniscule volumes of interface materials to liquefy and over extremely short times the materials flow together as viscous fluids to form interlocking waves. This takes place without causing significant local melting. In the case where intermetallics form from mixing of the base materials through plastic straining and shear stresses at a wavy interface, the thickness of the intermetallics is typically less than 2μm. In order for the

thickness of the intermetallic layer to exceed this length, voiding and local melting is likely needed. The intermetallic layer is the thickest in Figure 16 where voiding and evidence of local melting is most prominent, reaching around 4 μm.

Porous regions at the interface were also identified when the formation of a distinctive reaction layer was not as obvious. Figure 19 shows an SEM backscatter image of porous region in a weld formed with an impact angle of 15º. There is contrast between the region and the two base materials, but the contrast more closely matches Al. The region does not appear to have the same character as the intermetallic phases and has a greater thickness than is typically seen, with a maximum of 6 μm.

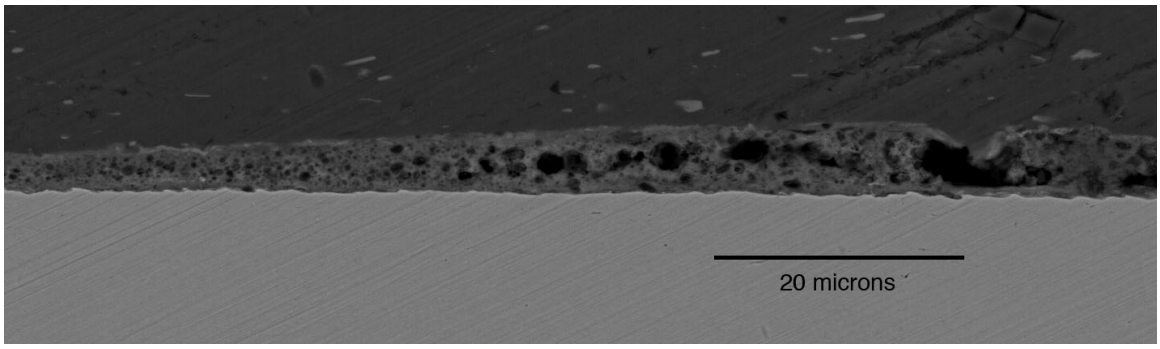

Figure 19: SEM BSE image of porous region in Al-steel weld formed with a 15º impact angle

Other interesting features indicative of local melting were observed in the same sample. Figure 20 shows damage to the steel substrate, possibly due to grain boundary liquation. Figure 21 shows another similar anomaly where the steel substrate appears to be damaged. Both porous regions indicative of local melting and resolidification and intermetallics are observed on either side of the damage.

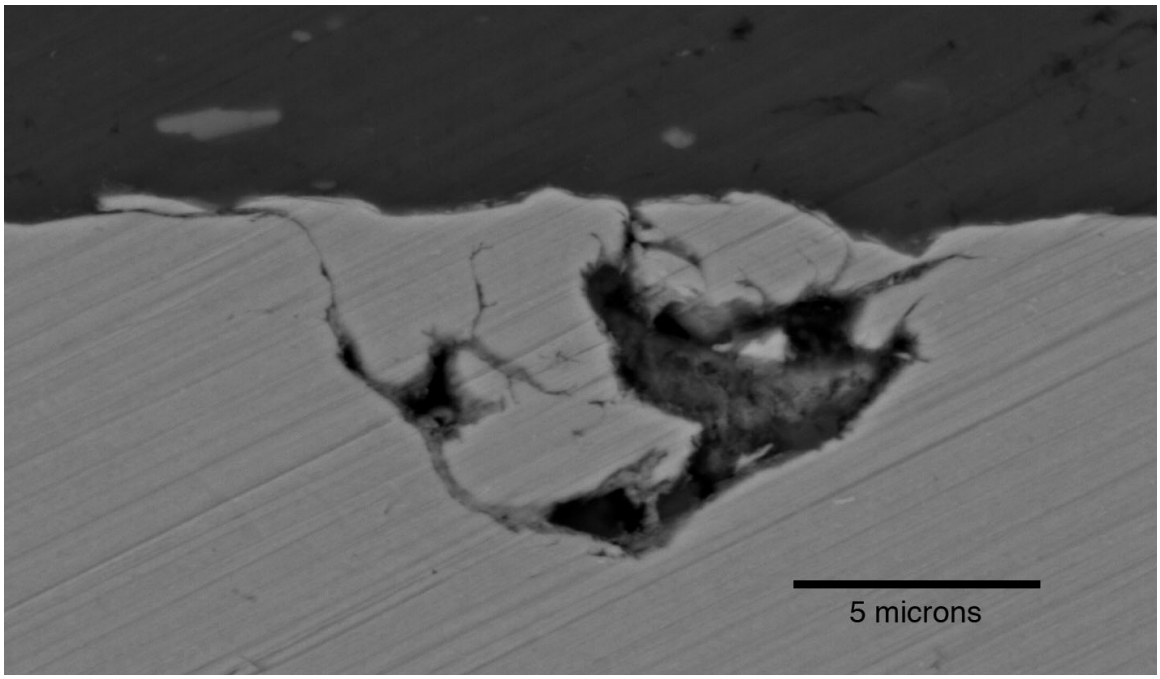

Figure 20: SEM BSE image of possible grain boundary liquation from local heating in 15º impact angle weld

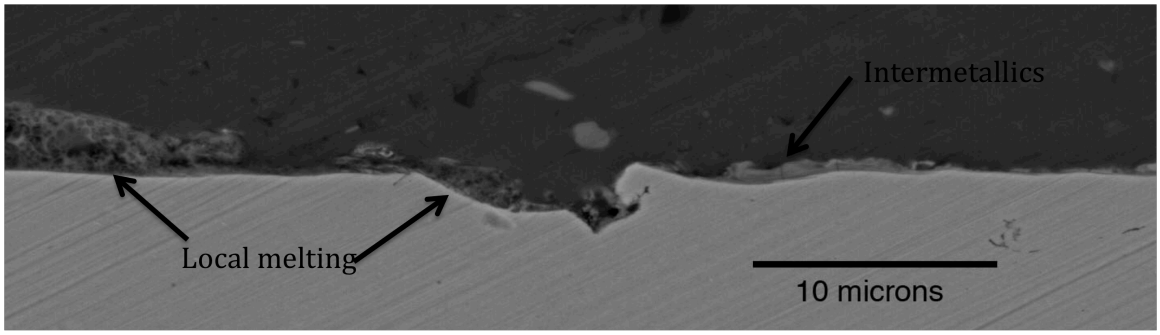

Figure 21: SEM BSE image of interface in 15º impact angle weld where porous regions characteristic of local melting and resoldification, intermetallics, and damage to the steel were observed.

Wavy/Straight Interfaces

It is well known that the less energy that is put into a system during collision welding, the smaller the wave amplitude and frequency will be. LIW typically results in waves of small amplitudes and the interface can be mostly flat. A wavy interface was not constant along the length of a weld. Instead, there were transitions between wavy and straight interfaces. Over the majority of the interface, a flat interface was typically observed. The yield strength of materials also plays a role in determining the wavy morphology, with higher yield strength materials resulting in smaller welds [15]. Steel is stiff and has a high yield strength, which also accounts for the flat nature of the interface, and the shallow waves when waves do appear. Figure 22 shows a weld produced at 13º that

exhibited shallow waviness for a portion of the interface and then transitioned back to a straight interface.

Figure 22: Wavy interface in 13º impact angle weld. On either side the interface returns to straight. 5% Nital etch.

To illustrate that similar waviness was seen over the range of impact angles, Figures 23-25 show SEM micrographs of the interface of a welds produced at 18º, 15º and 8º. The 8º impact angle weld interface features the same intermetallic region discussed above. Within these same samples also existed straight interfaces.

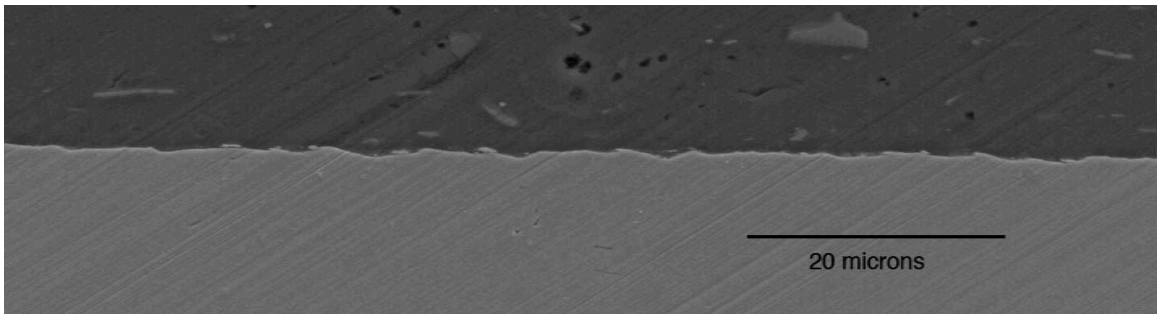

Figure 23: SEM SE image of wavy interface in 18º impact angle weld

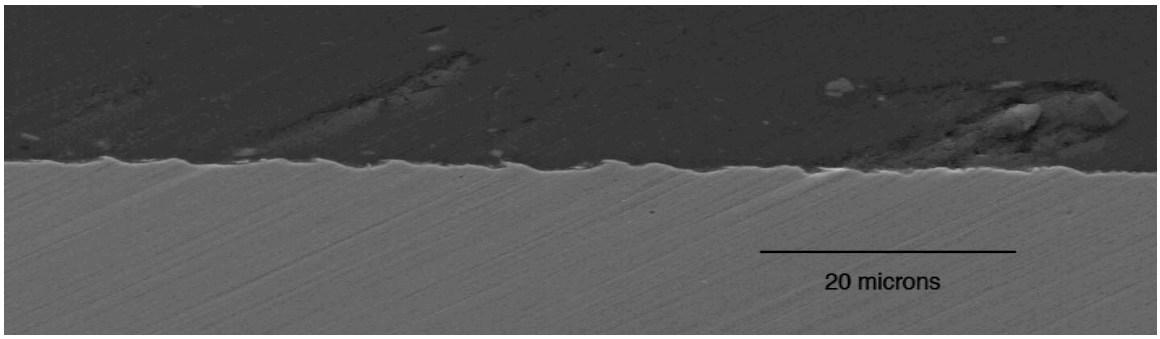

Figure 24: SEM SE image of wavy interface in 15º impact angle weld

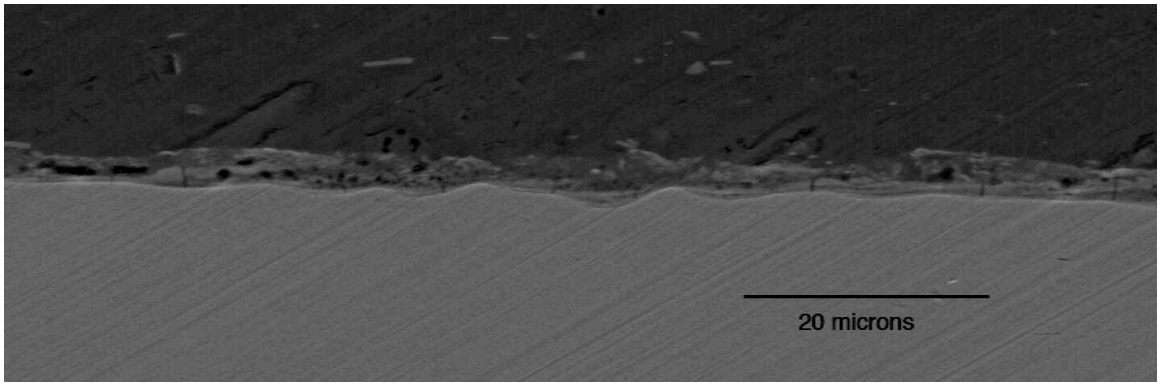

Figure 25: SEM SE image of wavy interface in 8º impact angle weld, featuring intermetallic reaction layer

Grain Refinement/Elongation

In order to determine the extent of grain refinement and surface deformation occurring at the weld interface, steel was lightly etched with 5% Nital to reveal the grain boundaries. In most cases, it appeared through optical microscopy that the steel grain structure was largely unaffected by the weld impact. Little grain refinement was seen that was different from surface effects of the steel manufacturing. In some cases, grain elongation was observed in the direction of the weld impact. Figure 26 shows grain elongation at the interface of a weld produced at a 15º impact angle. Figure 27 shows the cross section of a weld produced at 11º and both grain elongation (Figure 27 a) and lack thereof (Figure 27 b).

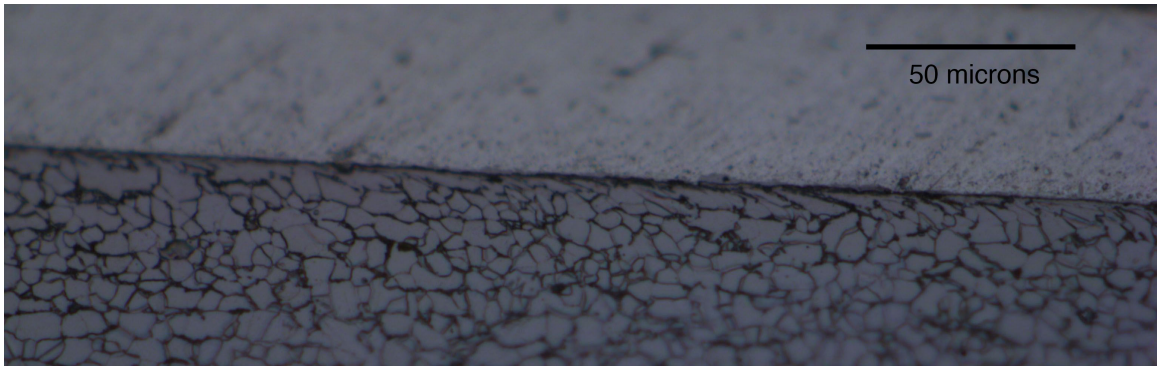

Figure 26: Steel rain elongation in weld created with 15º impact angle. 5% Nital etch.

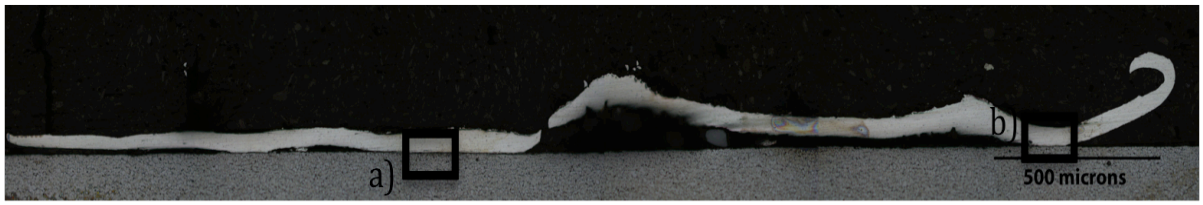

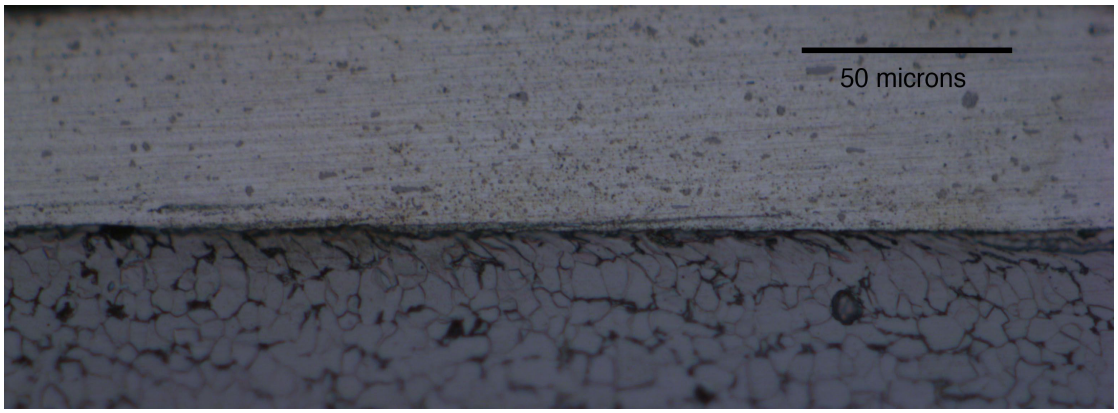

a)

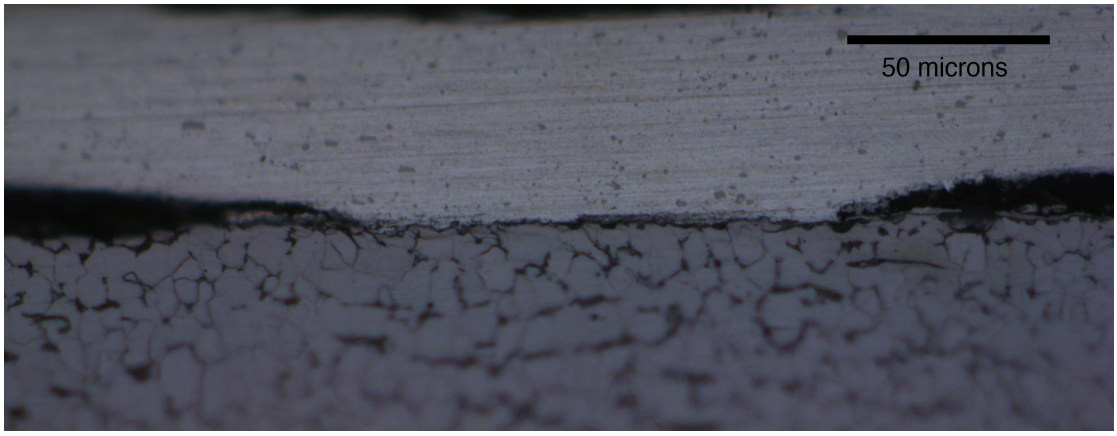

b)

Figure 27: Cross section of 11° impact angle weld a) steel grain elongation in weld direction b) lack of any grain deformation. 5% Nital etch.

Figure 28 shows what was typically seen at the interface of most samples. The grain structure for steel was similar to what was observed at the surface of an unimpacted region. The grains did not appear to be refined or elongated. Any refinement is likely due to surface effects from manufacturing.

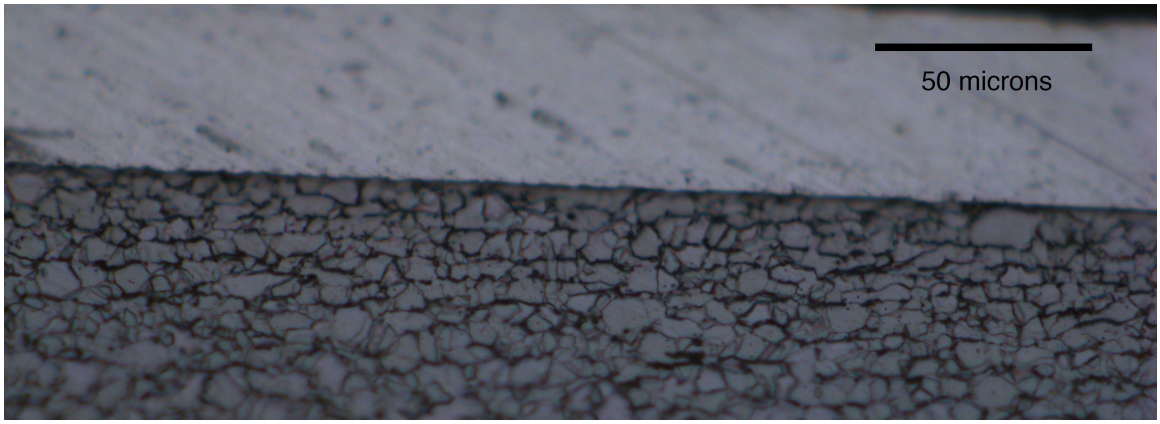

Figure 28: Lack of steel grain refinement or elongation in 15º impact angle weld. 5% Nital etch.

Hardness

Nanoindentation was performed on two samples, the 8º impact angle sample shown in previous SEM micrographs where a ~2μm thick intermetallic layer and voiding were found at the interface, and the 15º impact angle sample shown in previous micrographs with a porous region ~6μm thick due to local melting. Figures 29 and 30 show the two samples with hardness values in GPa overlaying the nanoindentation points.

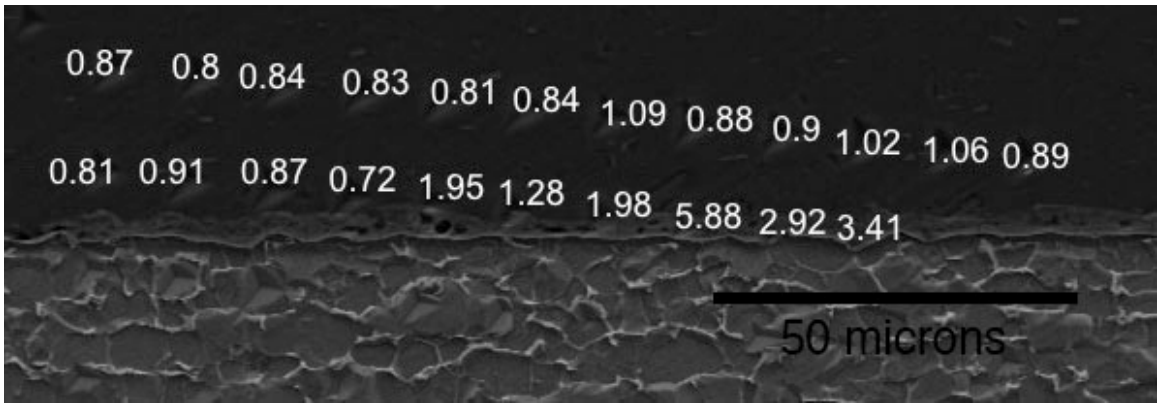

Figure 29: 8º impact angle sample with hardness measurments in GPa over the nanoindentation points

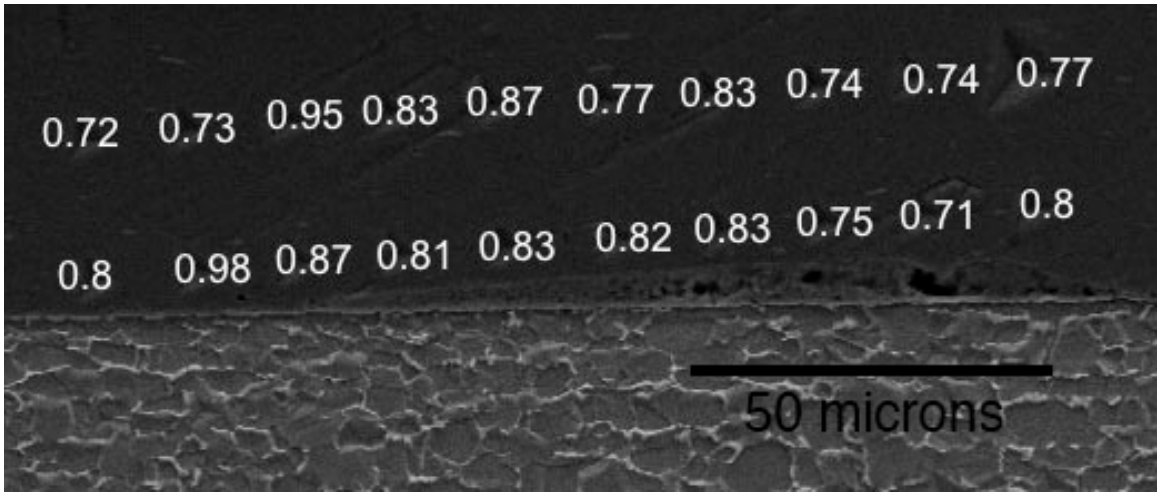

Figure 30: 15º impact angle sample with hardness measurments in GPa over the nanoindentation points

A control sample of the cross section of the Al foil was mounted and polished for nanoindentation. Over 40 indents, the average hardness was found to be 0.99 GPa with a standard deviation of 0.19 GPa. The average hardness of the aluminum in the 8º weld was 0.88 GPa with 0.09 GPa standard deviation. Intermetallics at the interface were significantly harder, with an average hardness of 2.9 GPa and a standard deviation of 1.64 GPa over 6 indents. The average hardness of the aluminum in the 15º weld was 0.81 GPa with 0.07 GPa standard deviation. Figure 31 shows the hardness readings as a function of distance from the interface.

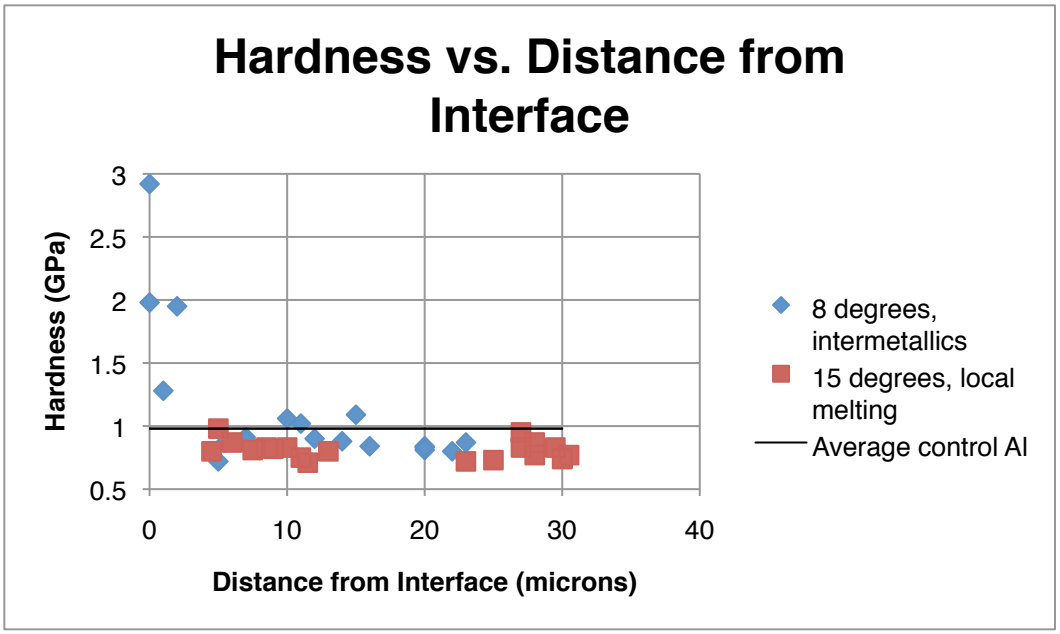

Figure 31: Hardness readings vs. distance from the interface in the 8º sample featuring an intermetallic region and the 15º sample featuring evidence of local melting. The average hardness value of the control Al foil is displayed as well.

Both samples showed on average reduced hardness compared to the Al foil control. This was different from what is normally observed in collision welding. Generally, hardness increases at the interface due to the refined structure from impact. Zhang et al. reported that in LIW, the hardened interface region on either side has a width of 20 μm [6]. These results are somewhat unexpected, but the foil was in the full hard temper, so an increase in hardness was not possible. The increase in temperature at the interface at collision likely caused annealing. The sample that showed significant evidence of local melting had the lowest average hardness. The 8º sample featuring intermetallics had an increase in hardness within microns of the interface due to those compounds, but the aluminum itself did not show any hardness increase as distance from the interface decreased. Still, the decrease in hardness was not drastic, especially considering the spread of the data and associated error bars. Overall, the mechanical properties of the base materials are maintained at the interface post collision.

High Angle/Low Angle Welds

In order to further determine if there was any effect on weld quality (jet entrapment, bulging of the flyer from the substrate, bonding) or interface microstructure due to impact angle, four low angle (8-9º) welds and four high angle (14-15º) welds were produced under the same conditions. Figure 32 shows the cross sections of the low angle welds, and beneath Figure 33 shows the cross sections of the high angle welds.

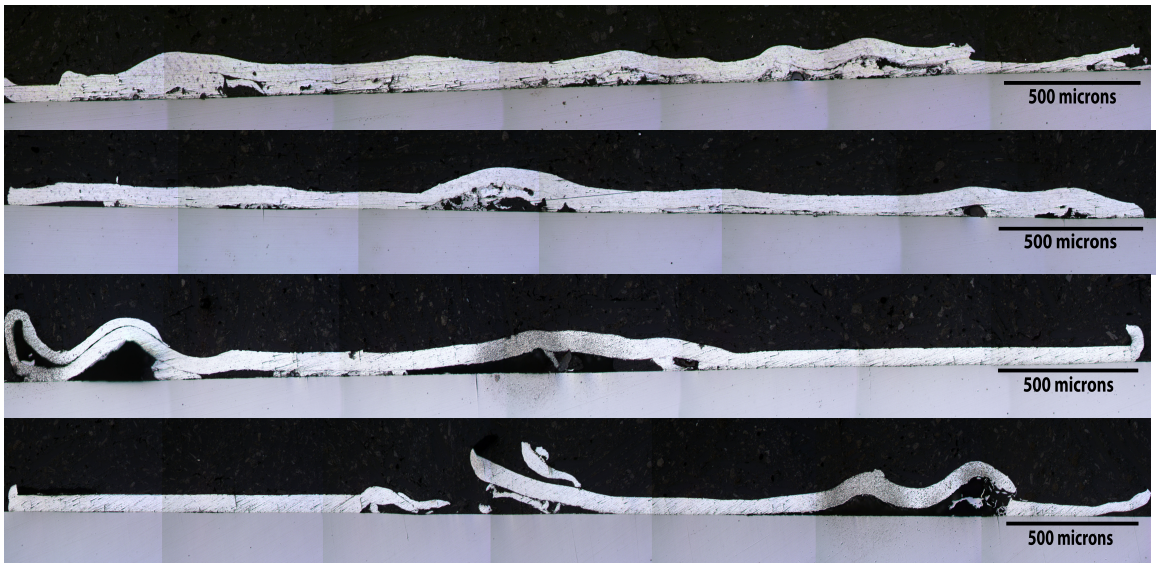

Figure 32: Cross sections of low angle welds

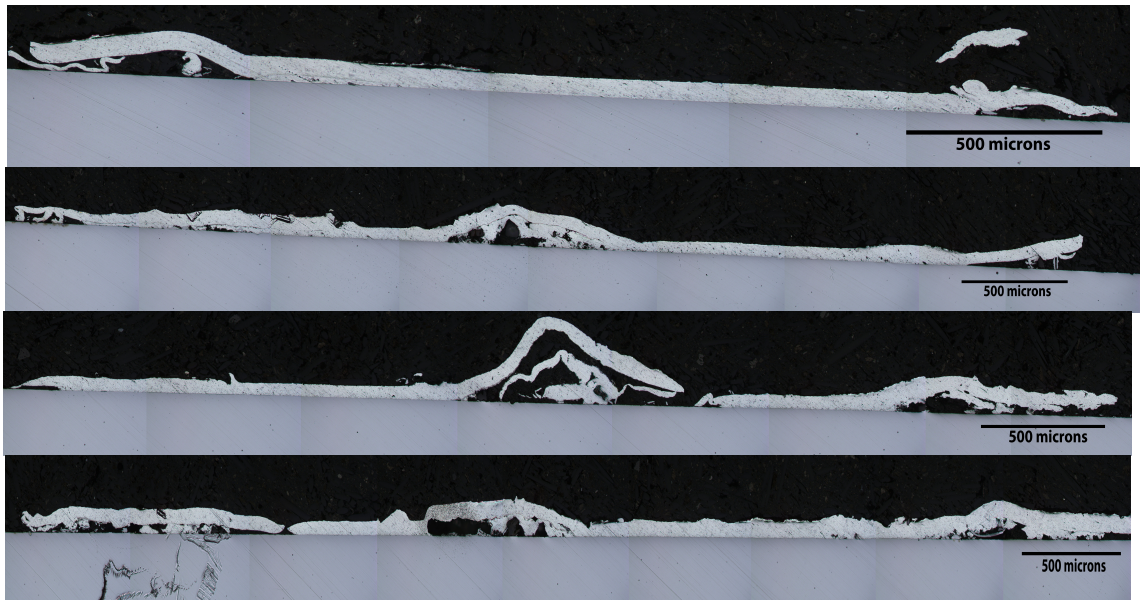

Figure 33: Cross sections of high angle welds

Comparing the cross sections within the groups, it can be seen that irregularity is occurring between welds created under the same conditions at close impact angles. Bulging, jet entrapment, spalling of the flyer and lack of intimate contact and bonding between the substrate and flyer are persistent problems in the welds. Reproducibility is an issue currently in LIW because of the hand-made set up. Because LIW is a new process in early development phases, there is a lack of standards in making the welds and there is not great control over the many variables during the methodology of creating the welds. There are no significant differences between the high and low angle welds that can be noted by

comparing the cross sections. Addressing the reproducibility issues would lead to a better understand of how impact angle affects the weld.

A variety of microstructural features were observed at the weld interface within a single sample. Figure 34 shows a weld cross section created at a low impact angle and the various features, including the wavy interface and thin intermetallic formation, jet entrapment and local melting and damage of the steel surface. Figure 35 similarly shows a weld cross section created at a high impact angle. At this interface waviness, thick intermetallic growth with voiding, and steel surface damage were observed.

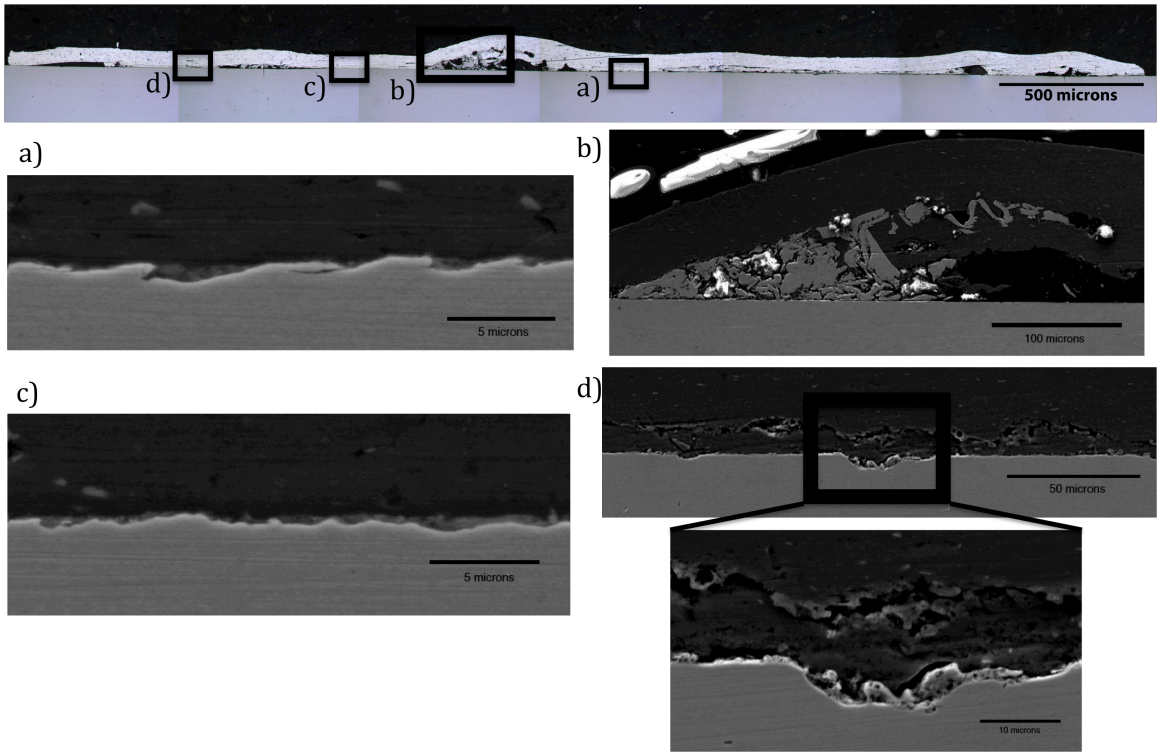

Figure 34: Low impact angle weld cross section with SEM micrographs of interesting microstructural features along the interface

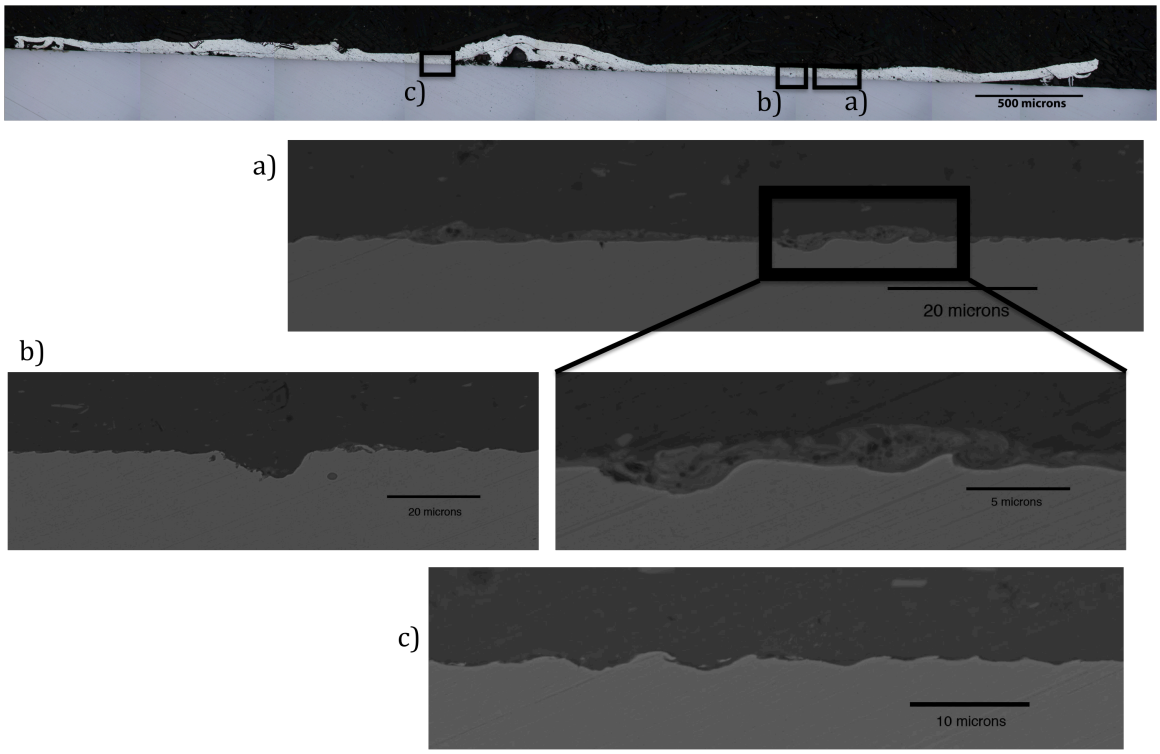

Figure 35: High impact angle weld cross section with SEM micrographs of interesting microstructural features along the interface

Heat Treatments

Heat treatments were performed on the welds to determine the response of the interface and to see how the collision process and interfacial microstructure would affect the course of interdiffusion. Eight high angle and eight low angle welds were prepared using the same conditions as described above. The high and low angle welds shown in Figures 32 and 33 serve as control samples to compare the heat treated samples to. Two high angle samples and two low angle samples were used for each heat treatment. There were four different heat treatments with time as the only variant. The heat treatments were performed at 600ºC for 1 hour, 2 hours, 8 hours and 16 hours. It was ultimately decided that impact angle was not a dominating effect in the weld character nor the heat treatment response, so a comparison is not presented. Figure 36 shows representative cross sections of the welds after each heat treatment.

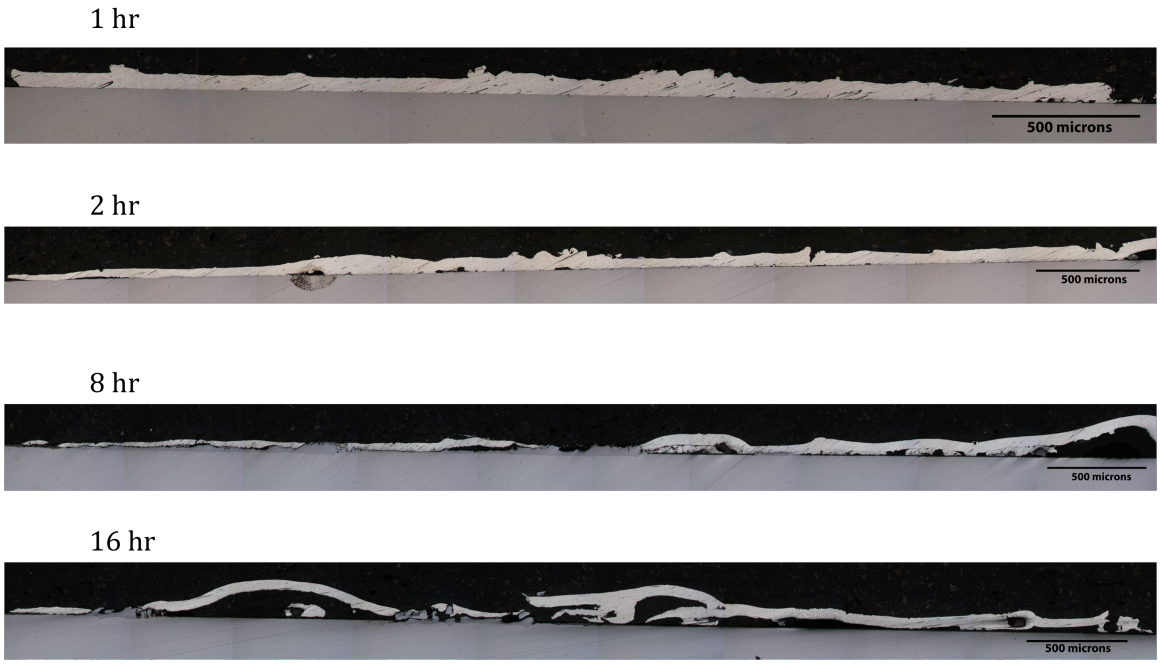

Figure 36: Representative cross sections of heat treated welds as time increases

After heat treating for 1 and 2 hours, the weld integrity was mostly maintained at what it was previous to heat treatment. After 8 hours, interdiffusion had consumed the aluminum flyer to the full thickness of the flyer in some regions. Because interdiffusion had occurred fully in some regions after 8 hours, there was not a significant increase in interdiffusion noted after 16 hours, but the weld continued to degrade with intermetallics causing brittle fracture and pushing the flyer away from the substrate.

Figures 37-42 show the various features seen after heat treatment for 1 hour. Figure 37 shows a thick intermetallic cluster, while Figures 38 and 39 show a continuously thin layer of intermetalllics similar to intermetallics that were seen prior to heat treatment, except no voids are present. In thick intermetallic layers, voids were generally present and it was likely that they formed from local melting and resolidification. In this case, it appears the thin, discontinuous intermetallics from impact have grown. Figures 40 and 41 show the evolution of a porous region following heat treatment, which appears to have a different character than the porous regions prior to heat treatment. Lastly, at some points along the interface there were no intermetallics observed. In these regions, there were neither intermetallics formed from impact nor from interdiffusion, as shown in Figure 42.

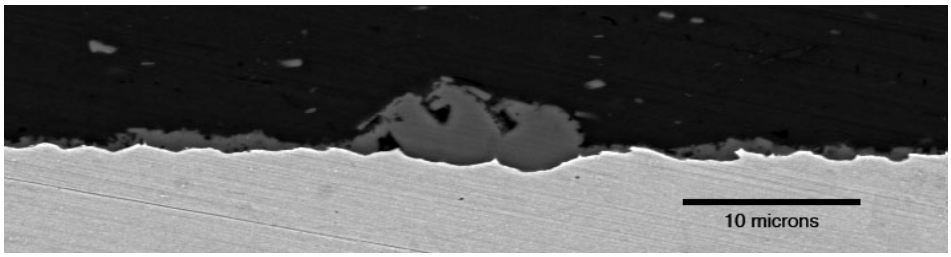

Figure 37: Thick intermetallic cluster in high impact angle weld heat treated after 1 hour

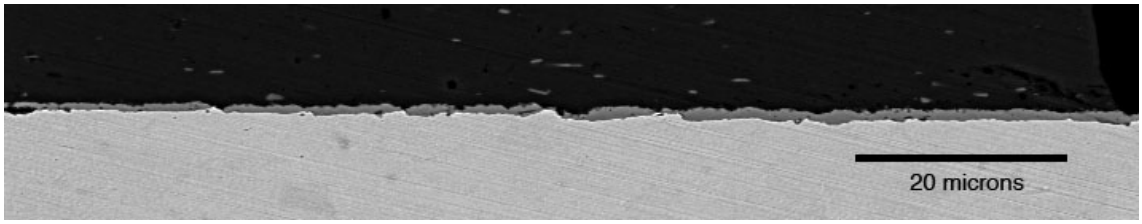

Figure 38: Thin intermetallic layer in low impact angle weld heat treated after 1 hour

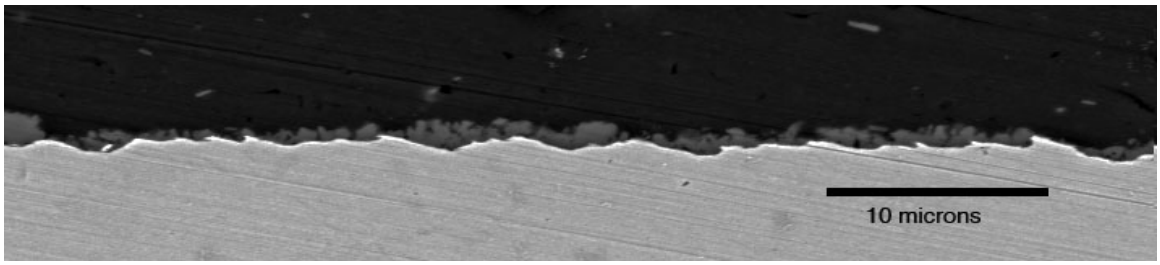

Figure 39: Another region of a thin intermetallic layer in low impact angle weld heat treated after 1 hour

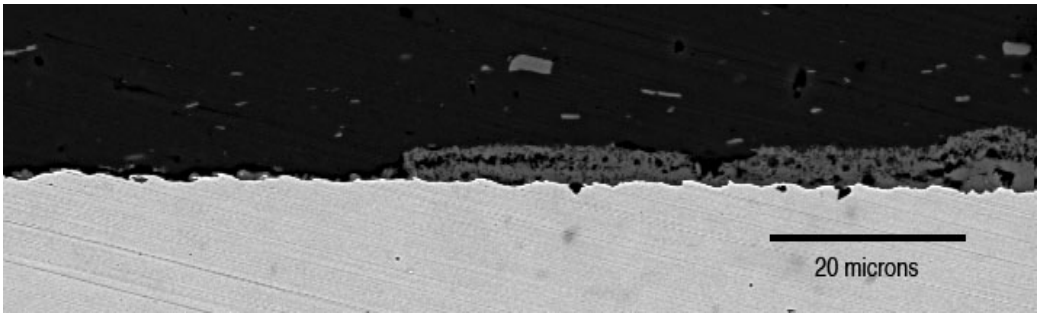

Figure 40: Porous region after heat treatment of 1 hour in low impact angle sample

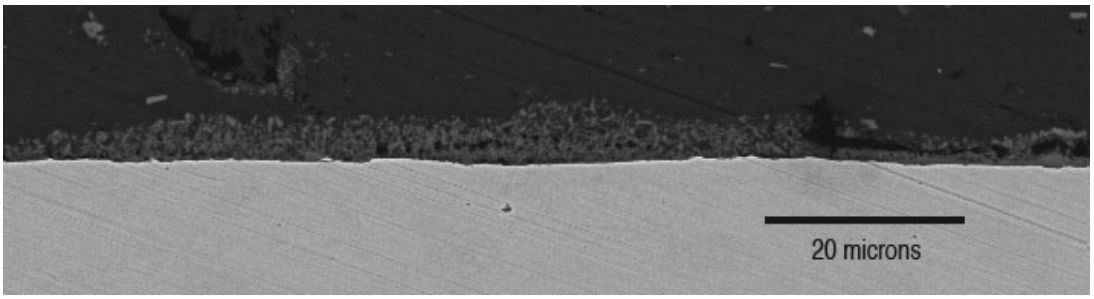

Figure 41: Second porous region after heat treatment of 1 hour in low impact angle sample

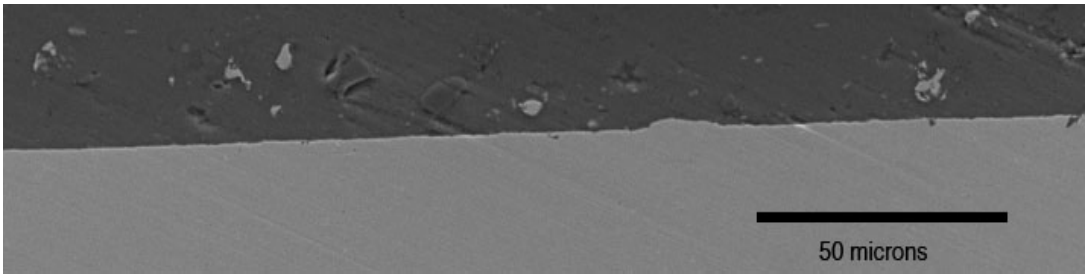

Figure 42: Interface from low impact angle sample showing no change, with no evidence of intermetallics either from impact or interdiffusion

Figure 43 below is a micrograph provided by Springer et al. that shows the phases at the interface following solid/solid interdiffusion for one hour between Al 99.99 and low carbon steel at 600ºC. There are two distinct phases, which appear to form a continuous layer that is generally the same thickness throughout. This 2-phase character or uniformity was not observed in these experimental results, meaning the interface from collision had an effect on the interdiffusion reaction. It is thought that the intermetallics formed from impact after 1 hour dominated and grew, and intermetallics from interdiffusion were likely not forming yet.

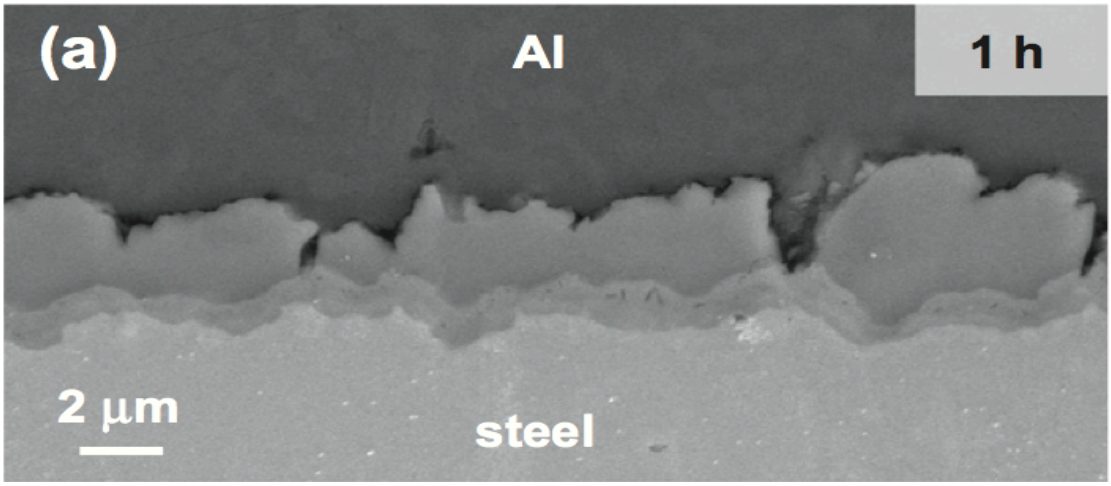

Figure 43: Interfacial phases after 1 hour of solid/solid interdiffusion between Al 99.99 and low carbon steel in literature [16]

Figure 44 shows a low angle weld cross section after 2 hours of heat treatment with various points highlighted to show the different reactions to the heat treatment. Similar to the 1 hour heat treatment, the response to heat treatment greatly varies along the interface. Some areas show little change (Figure 44 a), others show thin intermetallics (Figure 44 d) and intermetallics of varying thicknesses and of a different character from the thin intermetallics were observed as well (Figure 44 c and b).

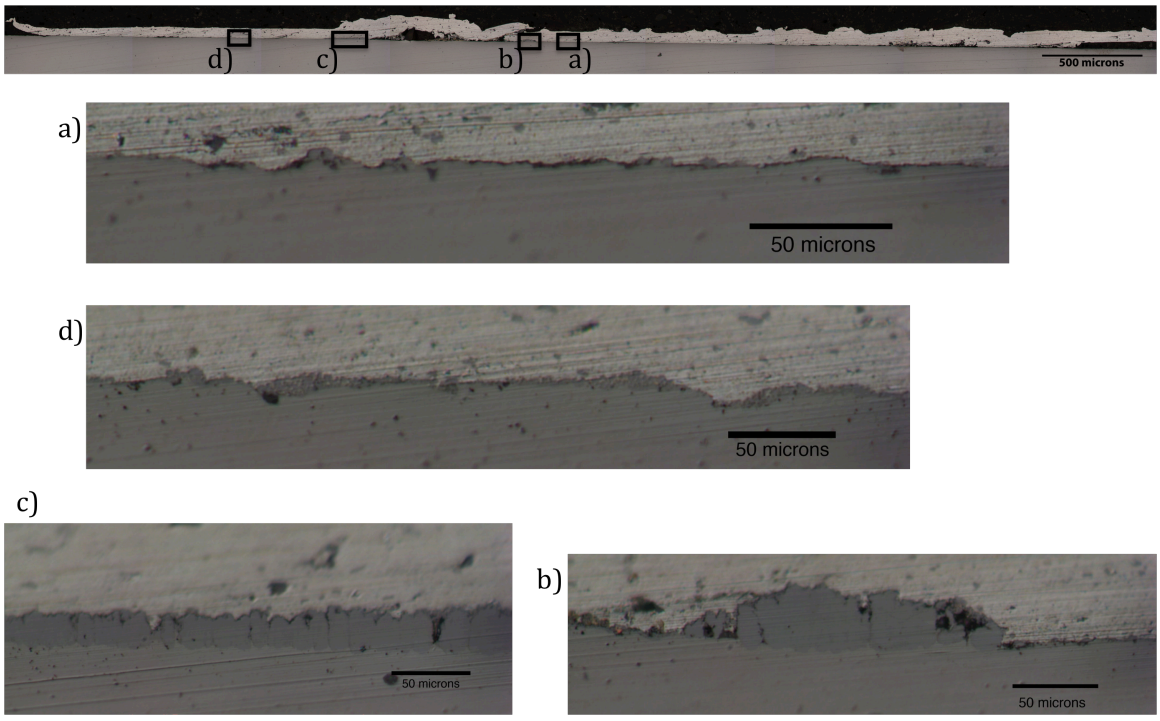

Figure 44: Low impact angle weld cross section after 2 hour heat treatment with a variety of reactions to heat treatment highlighted along the interface

Figures 45-48 show the various forms of intermetallics after the two hour heat treatment as revealed by SEM. Figure X shows thin intermetallics discontinuously distributed at the wave vortices. Figure X shows a layer of intermetallics that appears to be similar to intermetallics seen before. It is thought these were formed during impact and grew during heat treatment. Figure X shows an intermetallic layer of similar thickness to Figure X but appearing to be slightly different. It is possible these intermetallics formed upon heat treatment, not impact. Figure X shows thick intermetallics that appear to be the result of interdiffusion due to their different character.

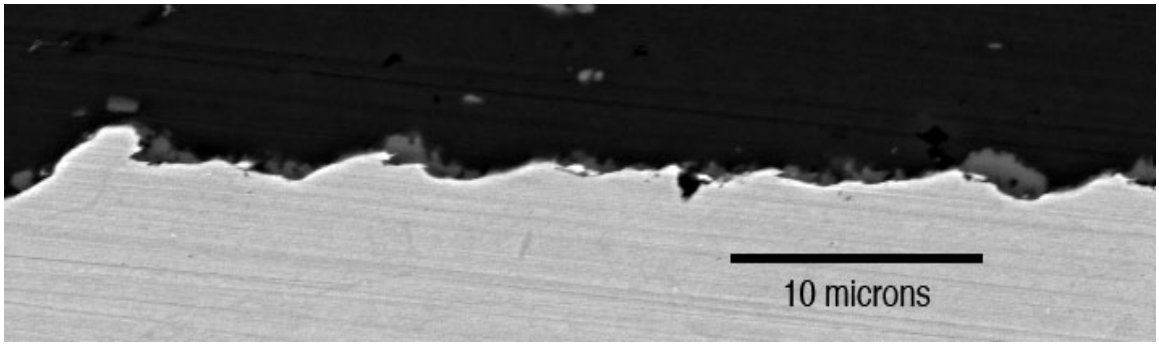

Figure 45: Discontinous pockets of thin intermetallics after two hour heat treatment in low impact angle sample

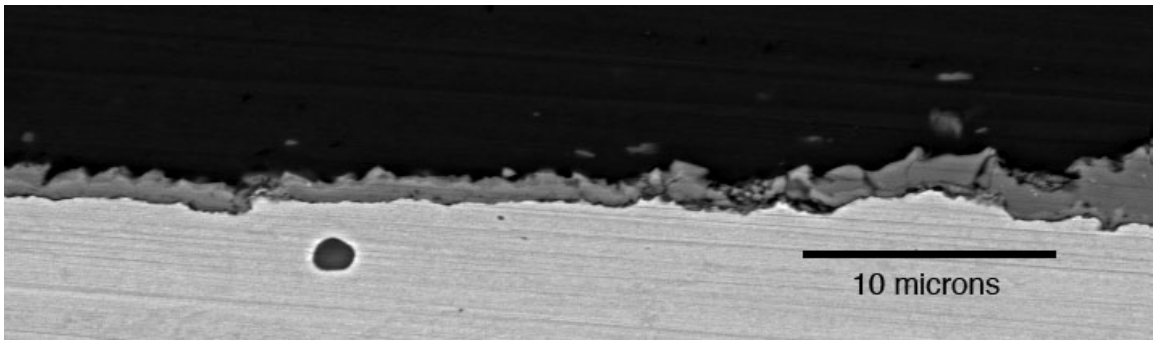

Figure 46: Thin layer of intermetallics in 2 hour low angle sample thought to have been the result of formation at impact that have since grown

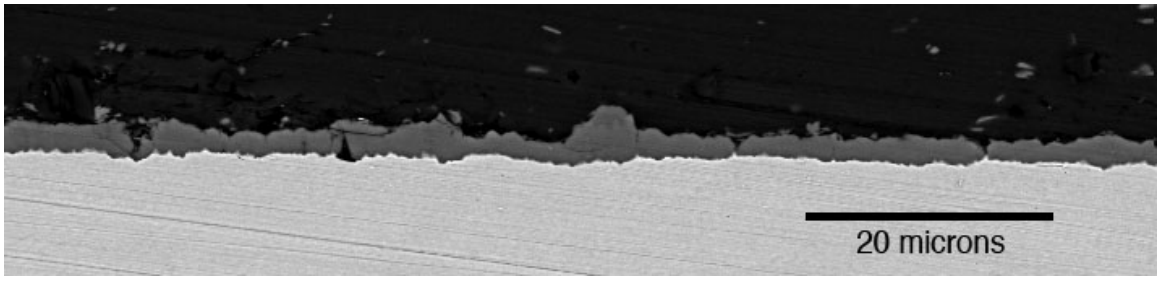

Figure 47: Thin layer of intermetallics in 2 hour low angle sample that may have formed from interdiffusion

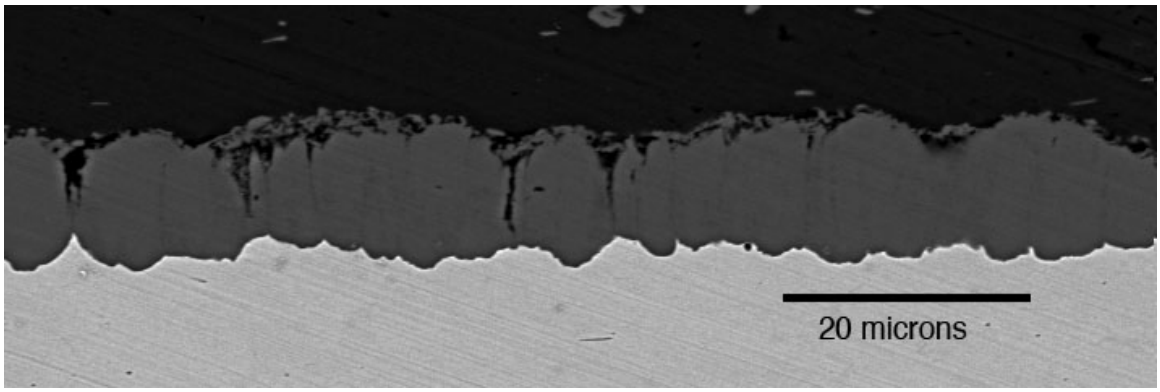

Figure 48: Thick layer of intermetallics after 2 hours in low impact angle sample that appear to be the result of interdiffusion

Figure 49 shows a weld cross section from a high impact angle sample after heat treatment of 8 hours with various points along the interface highlighted. After 8 hours, it appears one type of intermetallic dominates and this intermetallic is likely the result of interdiffusion. At some points, the thickness is small and uniform (Figure 49 c), other points have globular clusters of thick intermetallic (Figure 49 b) and in some regions the entirety of the thickness of Al is consumed by the intermetallic (Figure 49 d and e).

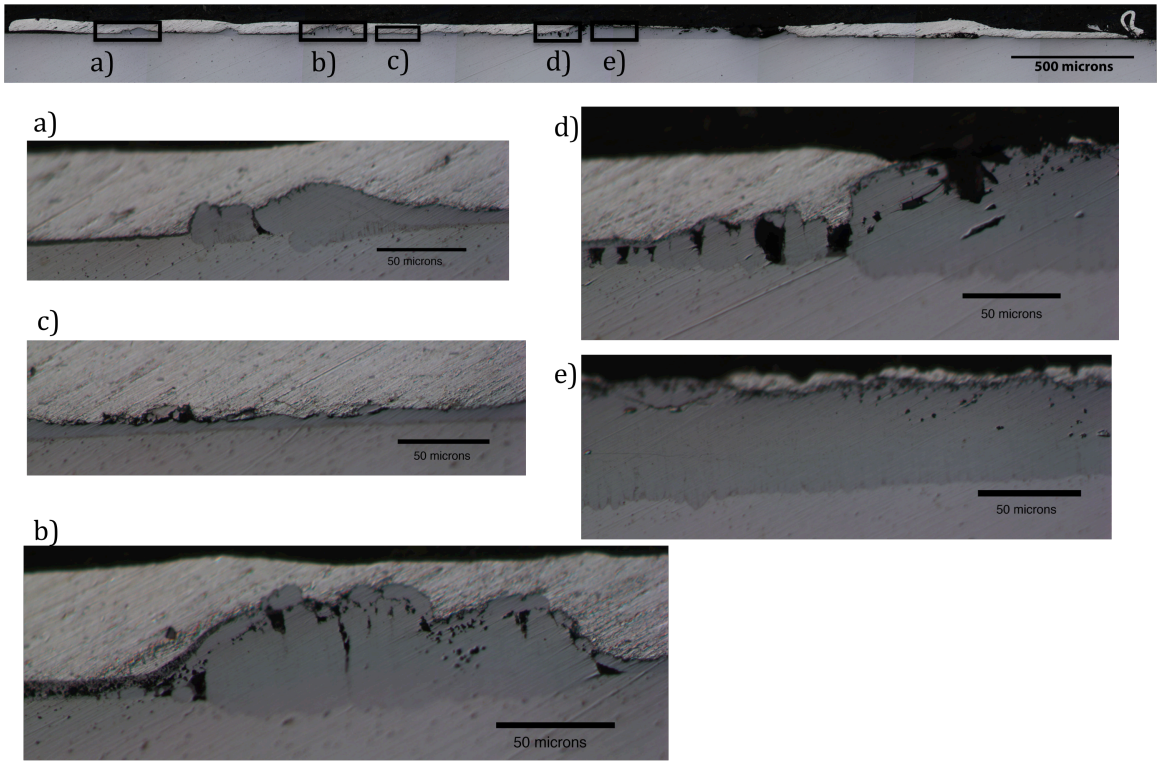

Figure 49: High impact angle weld cross-section after heat treatment of 8 hours with varying thicknesses of intermetallic formation highlighted along the interface

Since in some areas the intermetallic completely consumed the Al after 8 hours, progressing to 16 hours did not reveal significant change in intermetallic formation. However, examining these 16 hour intermetallics under SEM revealed interesting characteristics about the compounds. Since techniques such as EBSD and TEM to identify the phases were out of the scope of this present study, literature results of solid/solid interdiffusion between aluminum and low carbon steel were used for preliminary identification and to understand if the experimental results match with what is seen to result from purely interdiffusion. In the literature, the phases were identified using a variety of analysis techniques, including EBSD, EDX and SAD. Figure 50 shows the SEM micrograph of the intermetallic region on the steel side after interdiffusion of 16 hours and Figure 51 shows a color-coded EBSD phase map of the reaction zone after interdiffusion of 1 hour. The η phase was identified to be Fe_2Al_5, the β' phase was identified to be FeAl and the κ phase was identified to be $AlFe_3C$ [16].

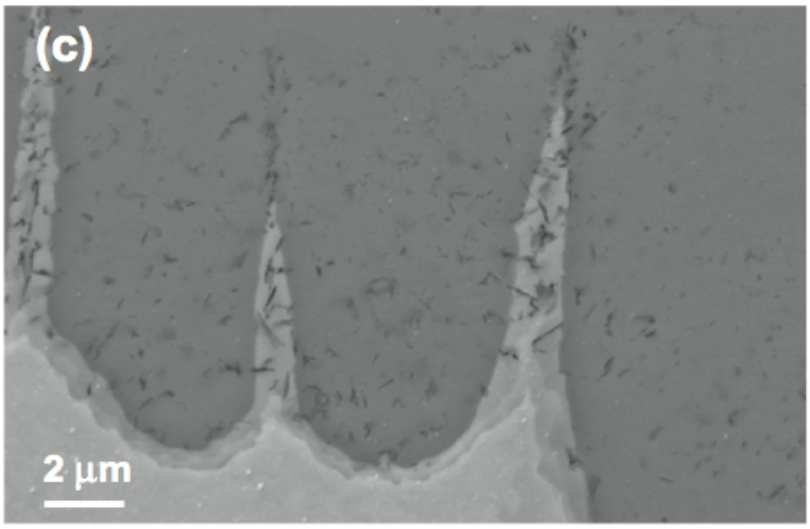

Figure 50: SEM micrograph after 16 hours of solid/solid interdiffusion between Al 99.99 and steel at 600ºC from literature [16]

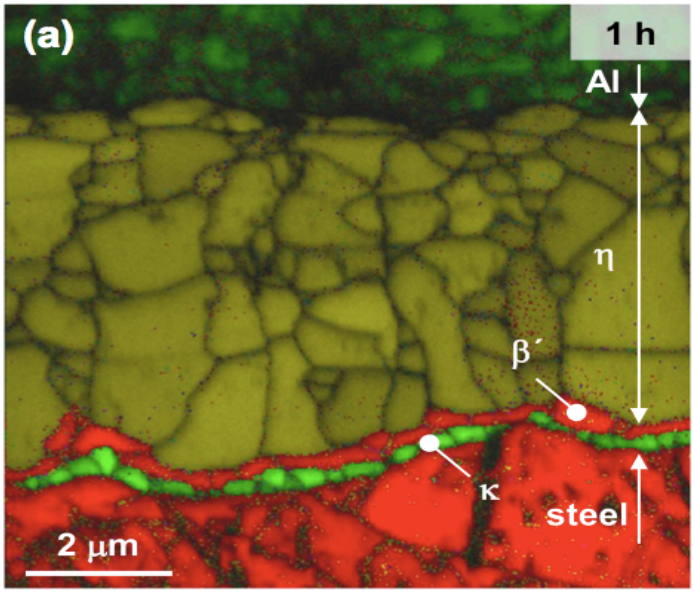

Figure 51: Color-coded EBSD phase map of reaction zone between steel and Al after solid/solid interdiffusion at 600ºC for 1 hour [16]

Figure 52 shows SEM micrographs of a high impact angle weld after heat treatment at 600ºC for 16 hours. The same thin phase is seen at the interface between the prominent intermetallic phase and steel as is seen in Figures 50 and 51 above. It is thus likely that this phase is both κ ($AlFe_3C$) and β' ($AlFe_3C$), and that the thick dominant phase is η (Fe_2Al_5). It is again apparent from this micrograph that the η intermetallic is not uniform across the interface, but is rather present in globular clusters. There is also an oxide layer present, which was identified because it formed on the surface on the steel in areas not in contact with Al. In this micrograph, it is interesting that there was alternating η intermetallic and oxide, indicating that within a small distance there was alternating metallurgical bonding with aluminum and areas where the bonding was not sufficient to allow for interdiffusion.

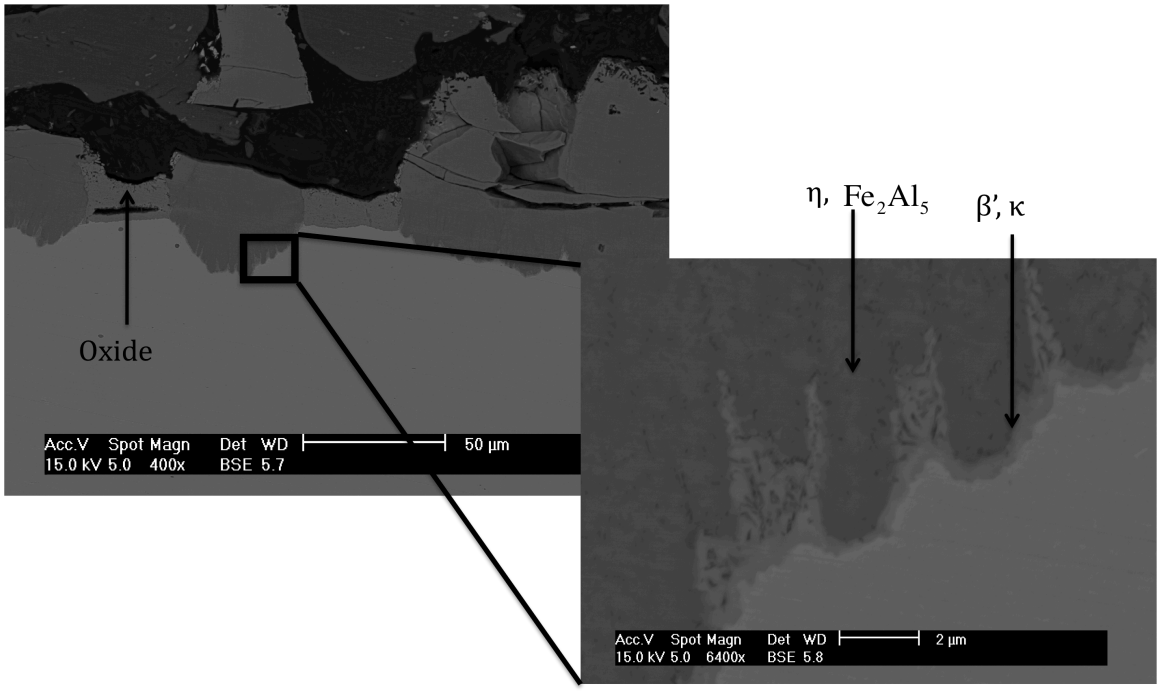

Figure 52: SEM micrographs of high impact angle sample after heat treatment at 600ºC for 16 hours with phases identified

Figures 53 and 54 show the η intermetallic at the aluminum interface. A faint continuous line of contrast can be seen within the intermetallic. The literature did not identify another phase present at the interface between η and aluminum. At present, it is not known if the contrast difference is truly due to a difference in compounds present, but this should be investigated as this could be another indication that the interface resulting from LIW reacts differently to heat treatment than a non-bonded diffusion couple.

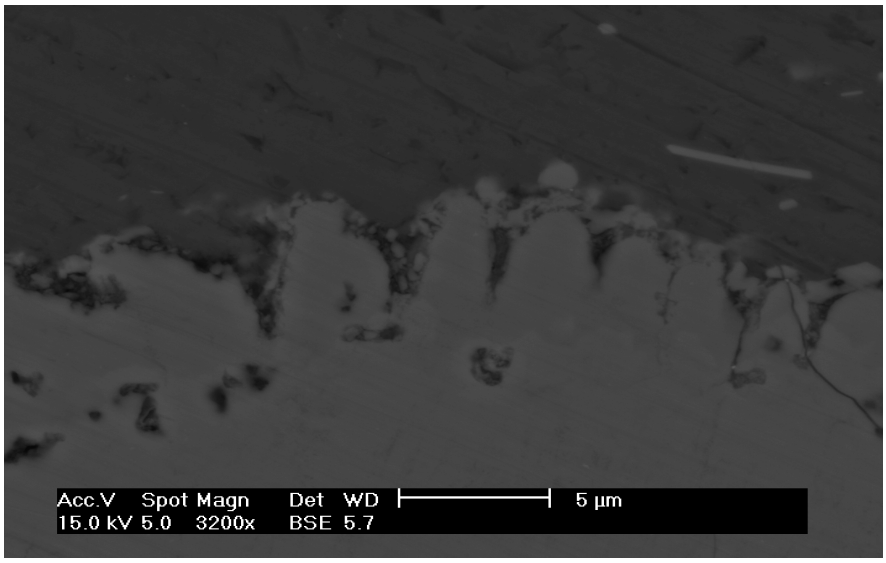

Figure 53: Interface between aluminum and η showing a faint contrast line in 16 hour low impact angle heat treatment sample

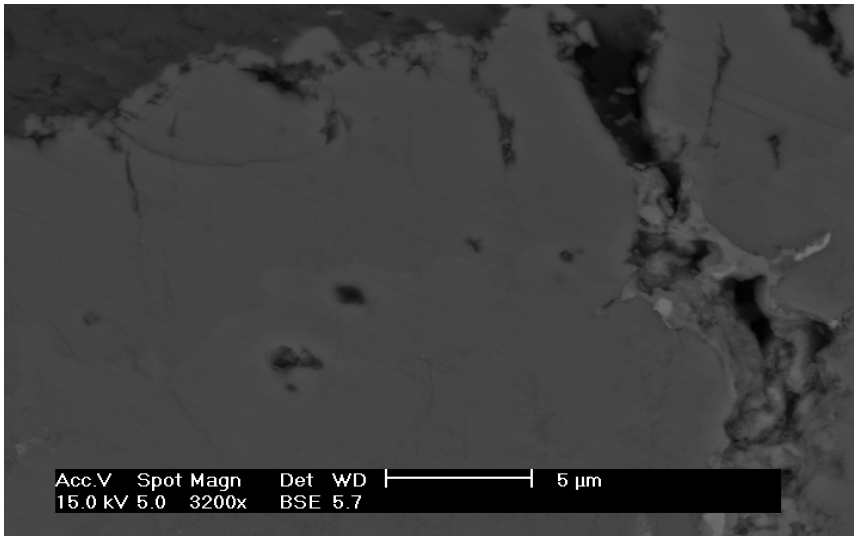

Figure 54: Interface between aluminum and η in another intermetallic showing a faint contrast line in 16 hour low impact angle heat treatment sample

As could be seen in the comparison of weld cross sections resulting from various heat treatment times, the 16 hour heat treatment led to degradation of the weld and increased spacing, or possible fracture between the flyer and substrate. Figures 55 and 56 show the brittle nature of the interdiffusion intermetallics. In these figures, the intermetallic has fractured and faceting can be observed.

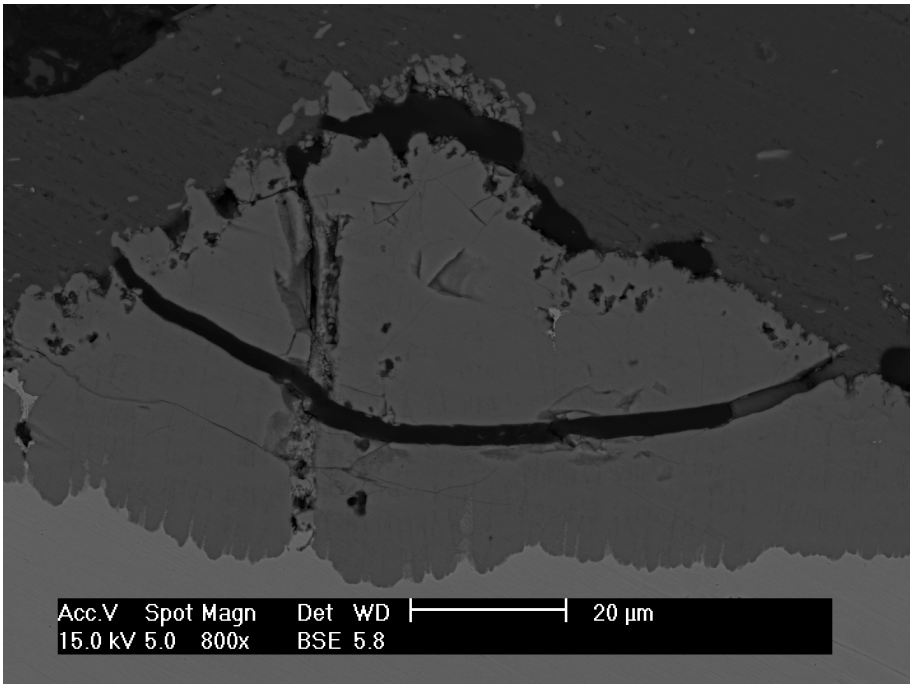

Figure 55: Brittle fracture of interdiffusion intermetallic in 16 hour low impact angle heat treatment sample

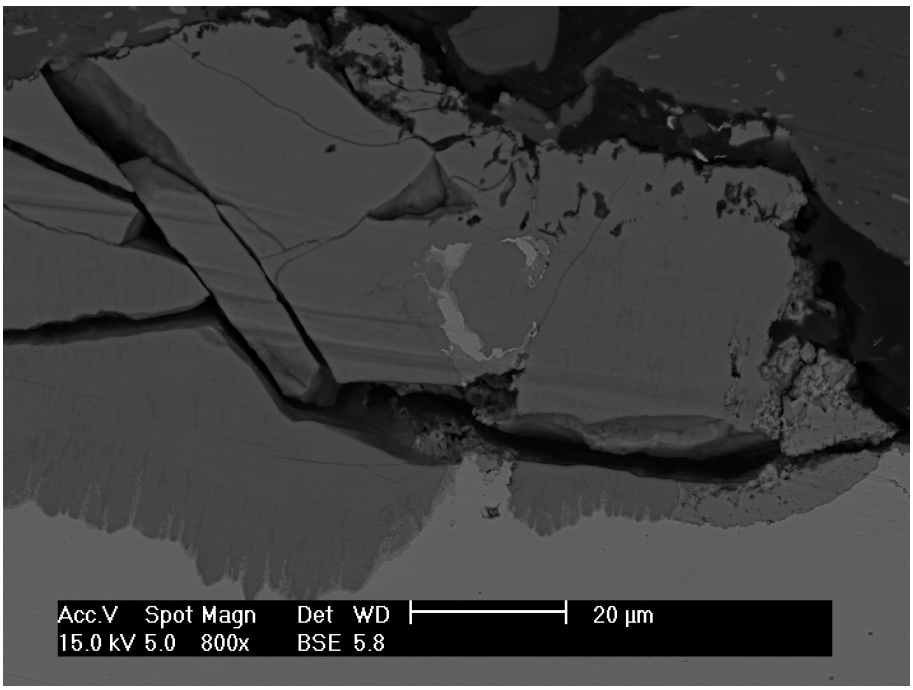

Figure 56: Brittle fracture of another interdiffusion intermetallic in 16 hour low impact angle heat treatment sample

It was also observed through the use of SEM that not all intermetallics had a thin distinctive phase at the interface with steel. Figure 57 shows a point on in the interface in a low impact angle 16 hour heat treatment sample where one

intermetallic cluster showed the thin phase, and another cluster that showed no thin phase. It seemed in the 8 and 16 hour samples, that the interdiffusion intermetallic consisting primarily of η dominated, but it is possible that this intermetallic that showed no thin phase at the steel interface is distinct from the η intermetallic and perhaps it originated from impact. More analysis is needed for identification, but this indicates that perhaps even at long heat treatment times there are other intermetallics present than the dominant η phase, and these could have been the result of another mechanism than interdiffusion. It is again interesting the variation in intermetallic thicknesses at roughly equal points along the interface.

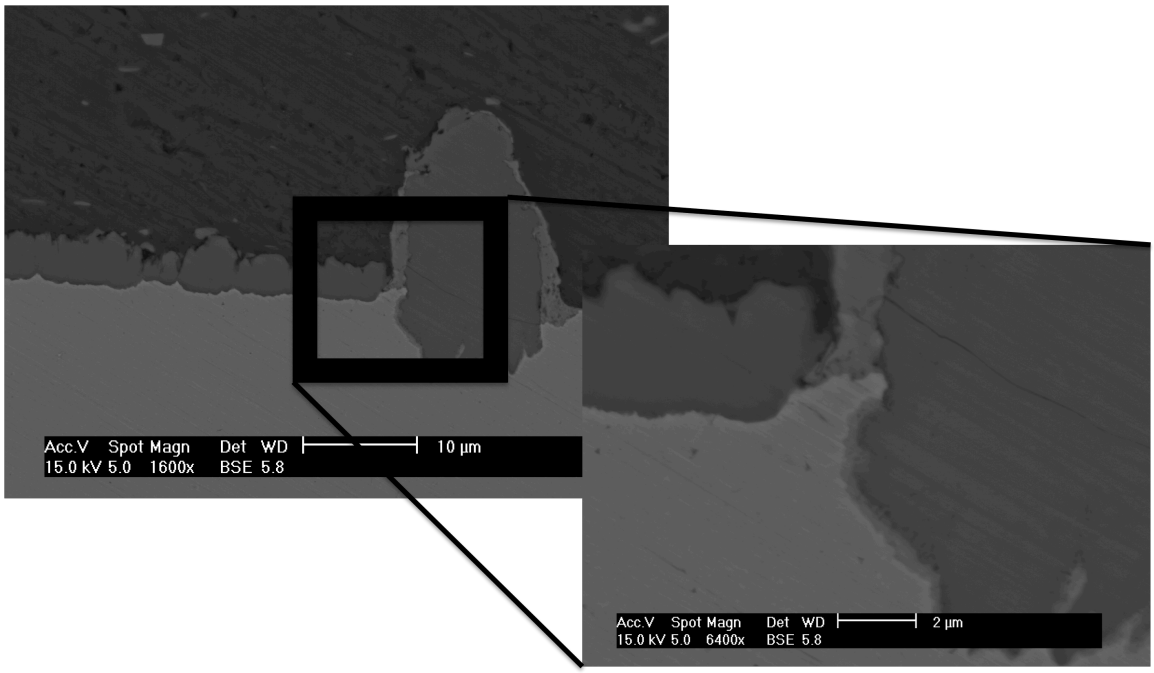

Figure 57: SEM micrographs from 16 hour low impact angle sample showing one intermetallic with thin phase at steel interface, and another without thin phase

Conclusions

Overall, this study was mostly an exploration and refining and standardizing the techniques will need to be done before drawing definitive conclusions. Through the exploration, the following are interesting findings to be further investigated:

•Nitro methane and other innovative set ups (new ink layers, confinements) could help in joining more difficult systems, though there may exist intrinsic limitations in terms of yield stress and hardness of the colliding materials and density of the flyer that will not allow all systems to be joined.

•New flyer configuration shown in Figure 3 was a simple and effective way of manipulating impact angle and bonding the whole interface. This set up can be used in the future with varying impact velocity and flyer thicknesses to generate welding windows

•Effective impact angle range for 0.002" Al under the described condition was ~7º-18º, with flyer entrapment and decreased bonding area concerns on the extremes of the range

•Flyer tearing was effected by impact angle, but no microstructural or weld quality patterns from impact angle were observed. Reproducibility must be improved to identify any patterns present, though impact velocity is known to have a more dominant effect on interface morphology/microstructure than impact angle.

•Intermetallics, voiding, local melting, waviness, grain elongation were all observed, but sporadically between and within samples.

- ▫Thick intermetallics and micro voiding observed together, suggesting local melting necessary to make thick intermetallics.
- ▫Local melting may be due to too small of laser spot size (higher energy density and impact velocity). This should be changed in future experiments.
- ▫Some mysterious steel damage (spalling, grain boundary liquation) was observed in several instances. This should be investigated.
- ▫The interface was mostly flat likely due to high yield stress/modulus of steel. Waviness was observed at various points along the interface.

•Hardness decreased from original full hard condition in control Al (more so in sample exhibiting local melting), and intermetallics at the interface were hard.

•In the 1 hour heat treatment, it is thought the intermetallics present were those that formed from impact and had grown.
    ▫The phases present did not match what was expected from interdiffusion literature.
    ▫In some cases no evidence of intermetallics was seen at the interface.

•In 2 hour heat treatment, several different types of reaction compounds were seen.
    ▫Possibly one intermetallic type was from impact and the other type from interdiffusion.
    ▫Distinction between two types of intermetallics means that intermetallics from impact were not the result of interdiffusion.

•In the 16 and 8 hour heat treated samples, the interdiffusion intermetallic dominated.
    ▫Matched well with literature expectations, but it is possible that more phases are present and first thin layer not always there.
    ▫The interdiffusion intermetallic was brittle, and the weld degraded from 8 to 16 hours

•Heat treatments may be good way of showing where true bonding occurred.

•It should be investigated why the thickness of intermetallics varies so greatly within a sample.

•Welds were extremely heterogeneous. Within a single weld many different features were present and between welds it was difficult to determine commonalities as conditions were kept the same.

•Work should be done on the reproducibility of welds before patterns in microstructure can be identified.

Future Work

•In the future, polish substrate to 1 μm.
•Repeat experiments using pure iron instead of steel to achieve a simple binary system.
•Perform low angle sectioning to cross-section the welds.
•Standardize procedures and make sure welds are reproducible before investigating microstructure further.
•Change the laser spot size to reduce impact velocity and limit local melting.
•Use cold mounting so no annealing of aluminum or steel occurs.
•Prepare a control couple for interdiffusion experiments.

•Use more advanced techniques, such as FIB preparation for SEM to identify phases.

References

[1] Zhang, Y., *Investigation of magnetic pulse welding on lap joint of similar and dissimilar materials.* The Ohio State University thesis, 2010.

[2] Daehn, G.S. and J.C. Lippold, Low temperature spot impact welding driven without contact, in 2009: U. S. 2009

[3] Wang, Huimin. "Laser Impact Welding and High Strain Rate Embossing." Electronic Thesis or Dissertation. Ohio State University, *OhioLINK Electronic Theses and Dissertations Center.*

[4] Pragnell, P., Haddadi, F., and Chen, Y.C., "Ultrasonic spot welding of aluminium to steel for automotive applications – microstructure and optimisation." Materials Science and Technolgy, 2011. 27(3). p. 617-624.

[5] Vivek, A., Hansen, S.R., Liu, B.C., Daehn, G.S., "Vaporizing Foil Actuator: A Tool for Collision Welding." Journal of Materials Processing Technolog, 2013. 213 p. 2304-2311.

[6] Zhang, Y., et al., Application of high velocity impact welding at varied different length scales. Journal of Materials Processing Technology, 2011. 211(5): p. 944-952.

[7] Bahrani, A.S., T.J. Black, and B. Crossland, *The Mechanics of Wave Formation in Explosive Welding.* Proceedings of the Royal Society of London.

[8] Palmer, T.A., et al., *Development of an Explosive Welding Process for Producing High-Strenght Welds between Niobium and 6061-T651 Aluminum.* Welding Journal, 2006: p. 252-263.

[9] Miles, J.W., *On the stability of heterogeneous shear flows.* J. Fluid Mech, 1961. **10**(4): p. 496–508.

[10] Vivek, A., Liu, B.C., Hansen, S.R., and Daehn, G.S., *Accessing Collision Welding Process Window for Titanium/Copper Welds with Vaporizing Foil Actuators and Grooved Targets*. Journal of Materials Processing Technology, 2014. 214: p. 1583-1589].

[11] Ben-Artzy, A., Stern A., Frage, N., Shribman, V., Sadot, O., 2006. Wave formation mechanism in magnetic pulse welding

[12] Alexander, D.E., G.S. Was, and F.J. Mayer, *Laser-driven micro-explosive bonding of aluminum films to copper and silicon.* Journal of Materials Science, 1988. **23**(6): p. 2181-2186.

[13] Dubrujeaud, B. and M. Jeandin, *Cladding by laser shock processing.* Journal of Materials Science Letters, 1994. **13**(11): p. 773-775.

[14] Barradas, S., V. Guipont, R. Molins, M. Jeandin, M. Arrigoni, M. Boustie, C. Bolis, L. Berthe, and M. Ducos, *Laser shock flier impact simulation of particle- substrate interactions in cold spray.* Journal of Thermal Spray Technology, 2007. **16**(4): p. 548-556.

[15] D. Liu, H. Wang, J.C. Lippold, G. S. Daehn, Laser Impact Welding for Joining Similar and Dissimilar Metal Combinations. Submitted to *Welding Journal* (2012).

[16] Springer, H., Kostka, A., Payton, E.J., Raabe, D., Kaysser-Pyzalla, A., Eggeler, G. “On the formation and growth of intermetallic phases during interdiffusion between low-carbon steel and aluminum alloys.” *Acta Materialia,* 2011. 59, pg. 1586-1600

[17] G. R. Cowan, O. R. Bergmann, and A. H. Holtzman, “Mechanism of bond zone wave formation in explosion-clad metals,” *Metall. Mater. Trans. B*, vol. 2, no. November, pp. 3145–3155, 1971.

[18] Ashby, MF. Materials Selection in Mechanical Design. Burlington, MA: Butterworth-Heinemann; 2005

[19] Watson, S., and Field, J. E. 2000. Integrity of thin, laser-driven flyer plates. *Journal of Applied Physics* 88(7): 3859-3863.